

A Comprehensive Calibration and Validation Site for Information Remote Sensing

**C. R. Li, L.L. Tang, L. L. Ma, Y. S. Zhou, C. X. Gao, N. Wang,
X. H. Li, X. H. Wang, X. H. Zhu**



- **Key Laboratory of Quantitative Remote Sensing Information Technology, Chinese Academy of Sciences, Beijing, China**
- **Department of Earth Observation Technique Application, Academy of Opto-Electronics, Chinese Academy of Sciences, Beijing, China**

8 Sep, 2015

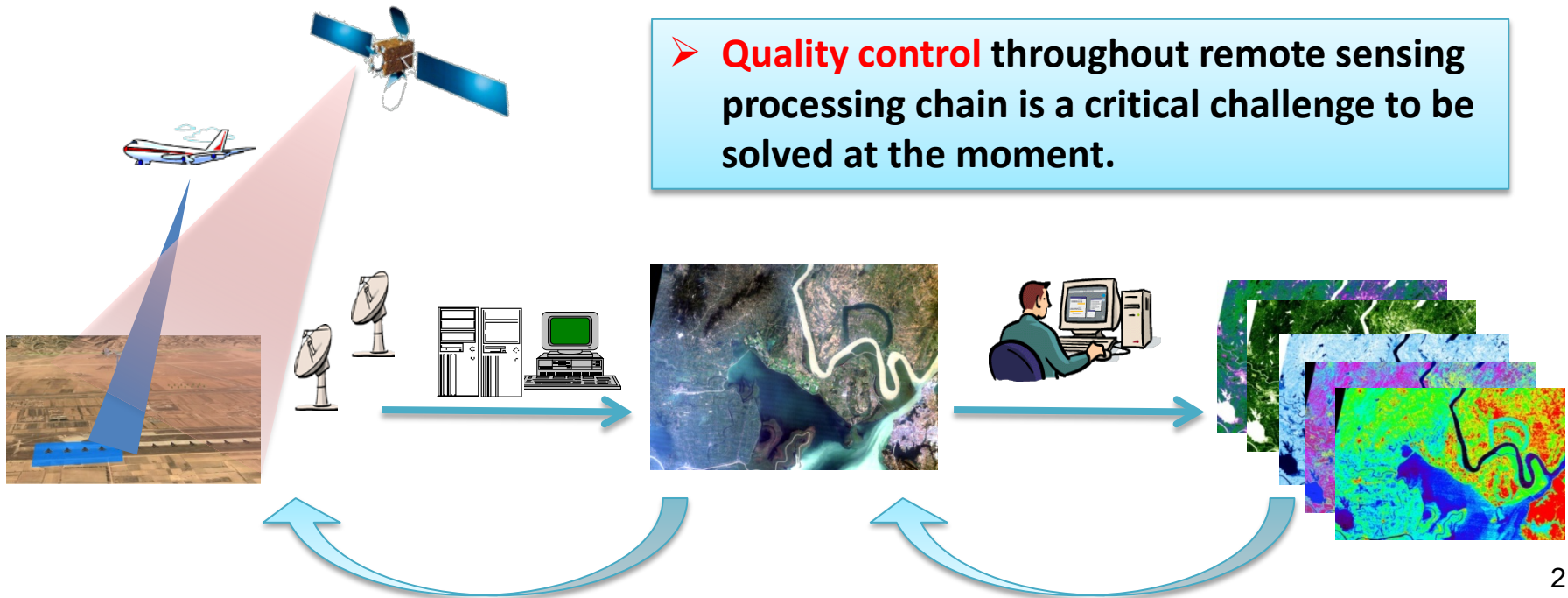


➤ Remote Sensing (RS) is principally an information business. **High-resolution** makes it possible to provide public with more universal information.

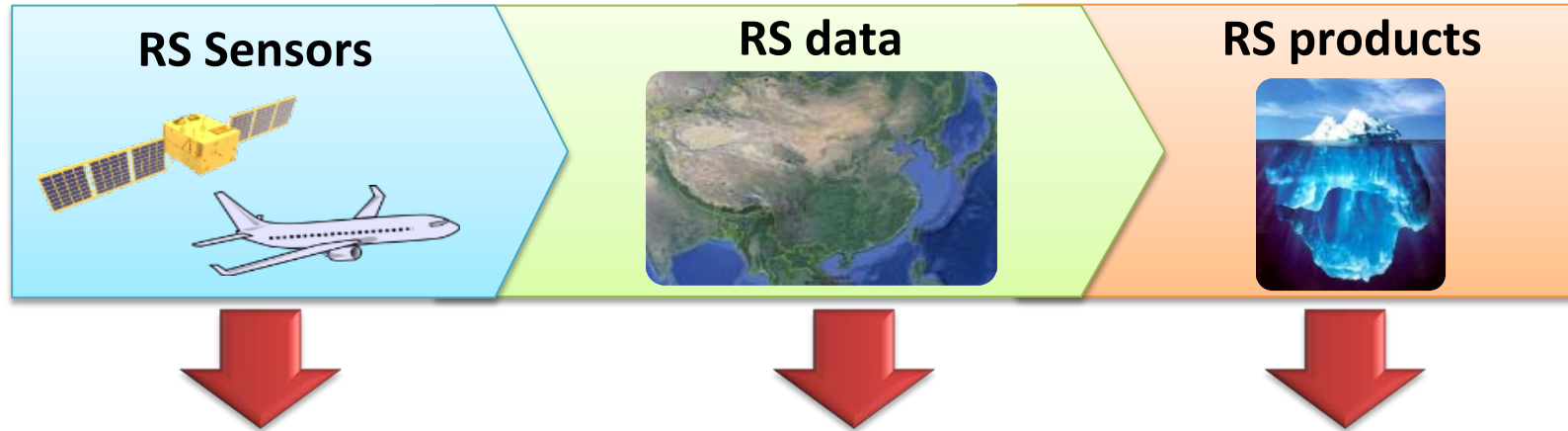


➤ **Precision and Accuracy** are the basic elements for RS products to lead the market.

➤ **Quality control** throughout remote sensing processing chain is a critical challenge to be solved at the moment.



Quality Control



Calibration Accuracy

- How to analyze the uncertainties in the whole calibration chain
- How to reduce those uncertainties

Benchmark Consistence

- How to ensure the long-term stability of ground reference targets
- How to ensure the comparability of the different sites
- How to ensure the comparability of different field measurements

Product Quality Traceability

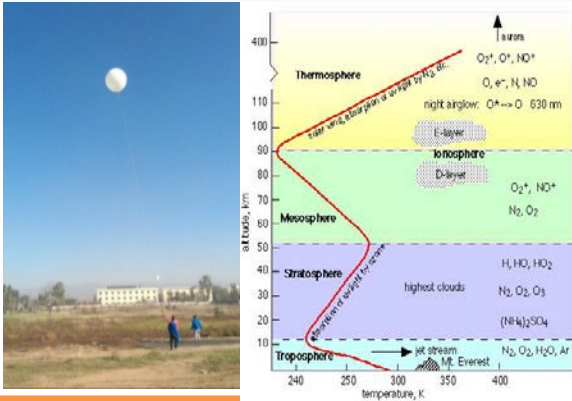
- How to understand the relationship of different performance
- How to develop a comprehensive site served for multi-performance assessment of different sensors that used to retrieve the same RS products.



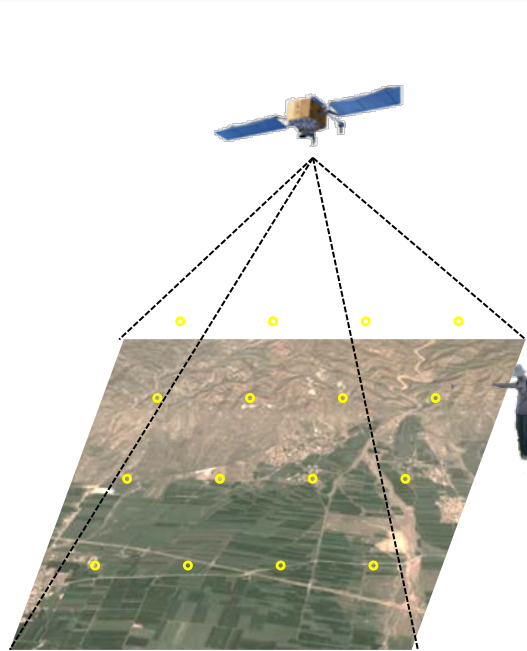
Calibration Accuracy

- The difficulties in accurately measuring temporal-spatial variation factors;
- The scaling gap between satellite and field observations;
- The scientific problems of accurate radiative transfer process description in a complicated Earth-atmosphere system

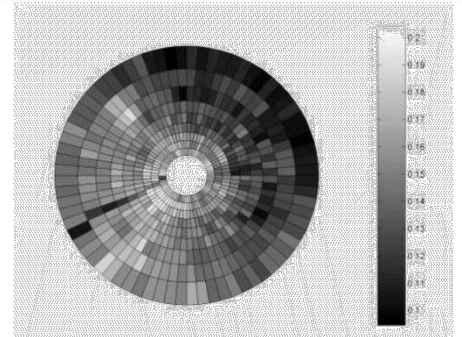
Difficult to measure the atmosphere due to the significant variation



Mismatching in temporal, spatial, angular and spectral scales of the ground v.s. satellite observations

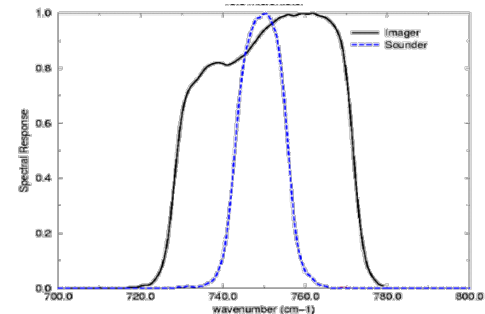
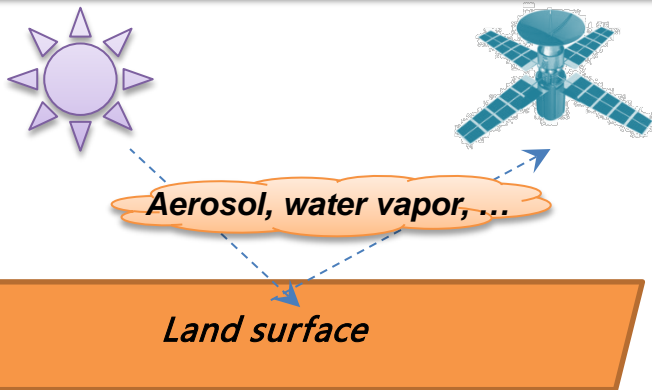


Temporal-spatial differences



The angular effect of surface radiation

Uncertainties in the modeling of atmospheric radiative transfer process



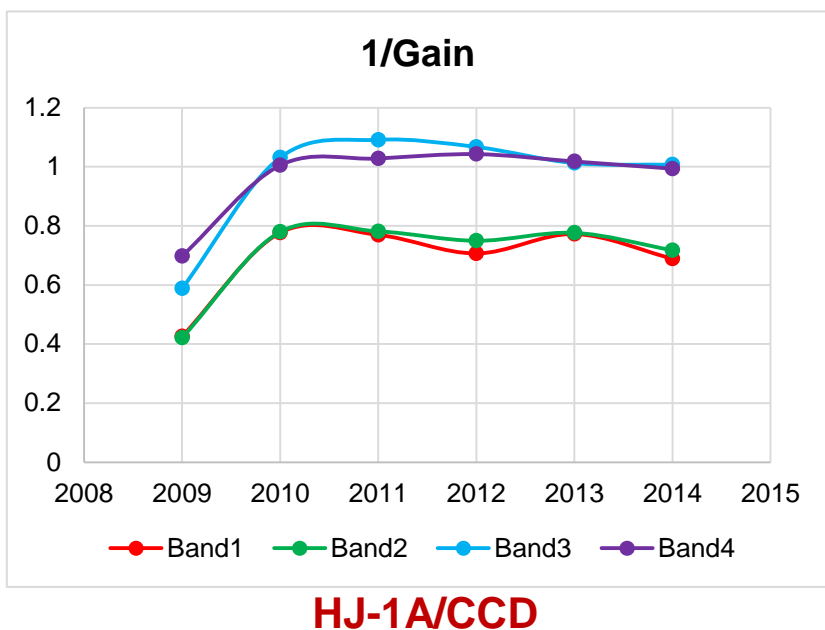
Spectral mismatching of different instrument



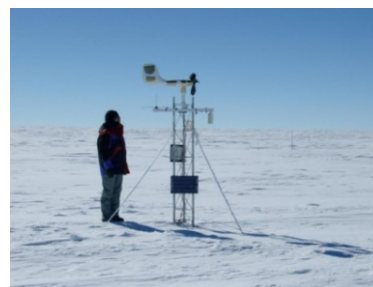
Benchmark Consistence

- High-frequency vicarious calibration technology;
- Ground targets with stable and significantly different characteristics;
- The standard measurement and data processing flow.

Low calibration frequency (once per year) is difficult to describe the sensor performance degradation.



Natural scenes hardly provide sufficient reflected/emitted differences to cover the wide dynamic range of the sensor in a limited imaging area.



DOME C



La Crau, FR



Rice field, CA



Walker Lake, NV

3

Product Quality Traceability

- The quality of RS information product is described by various quality metrics. Calculating different quality metrics of different sensors requires different ground reference targets.
- Quality metrics for characterizing the RS sensor performance are usually highly correlated with each other. High resolution make it possible to assess all the quality metrics in one site.

Image resolution

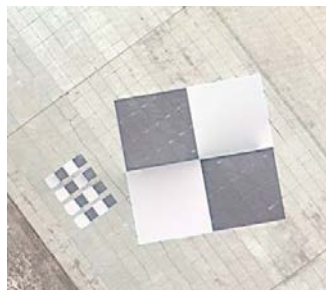


Tri-bar target



Fan-shaped target

MTF assessment

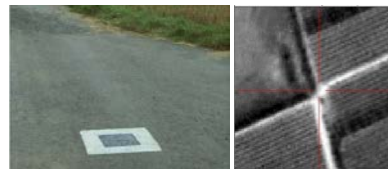


Edge target

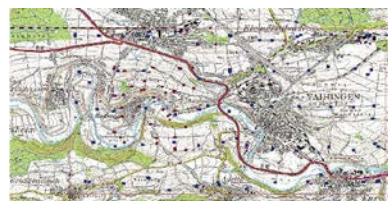


Point target

Geometric assessment



Artificial/natural control points



Geometric calibration test field

SAR quality assessment



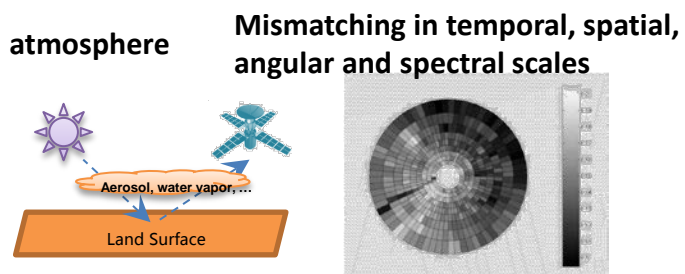
Passive targets



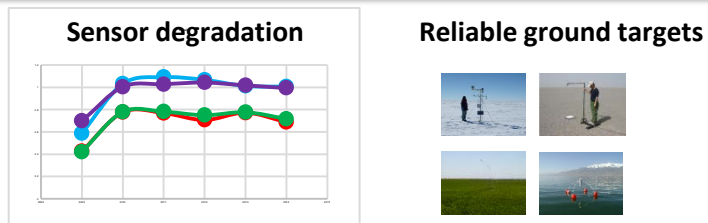
Active targets

Summary

Calibration Accuracy



Benchmark Consistence



Product Quality Traceability

Comprehensive targets for various product quality assessment



Comprehensive Cal&Val site

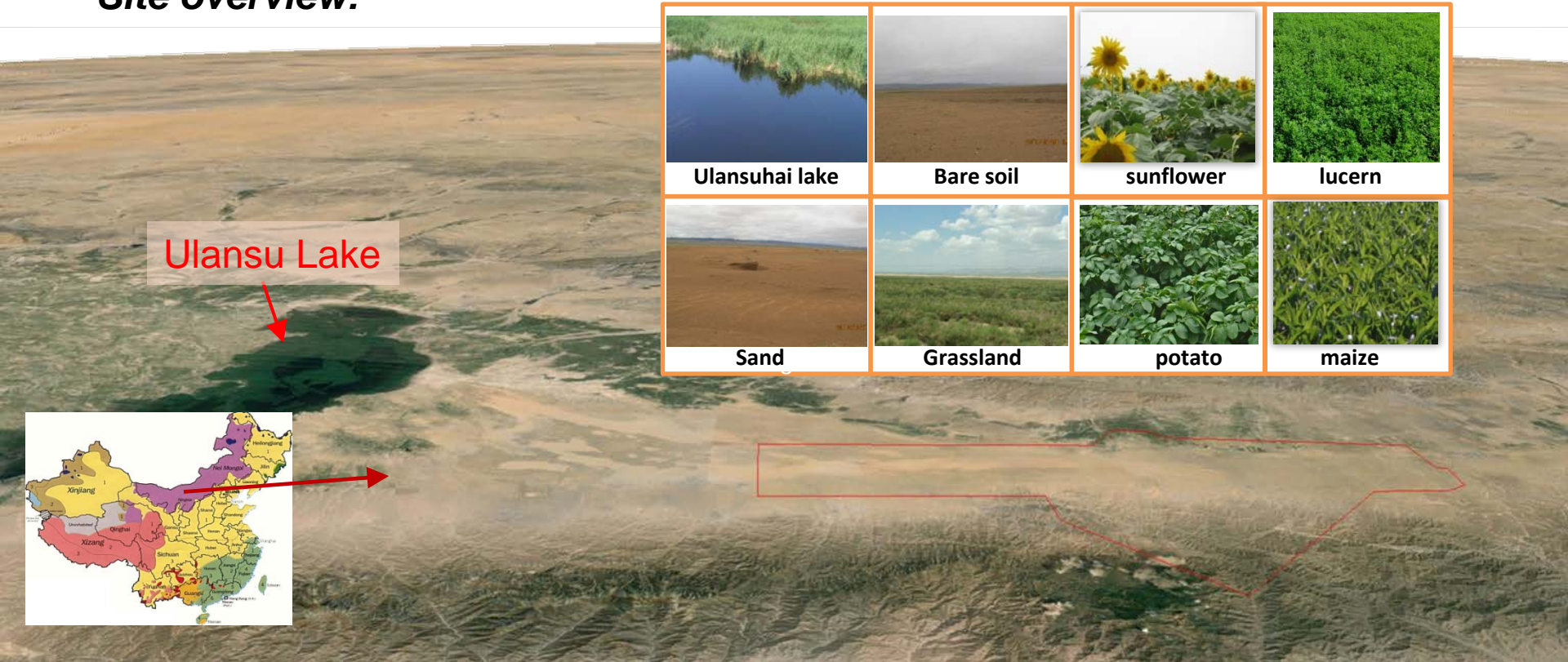
High-stable ground standard targets

High-accuracy stepwise Cal&Val system

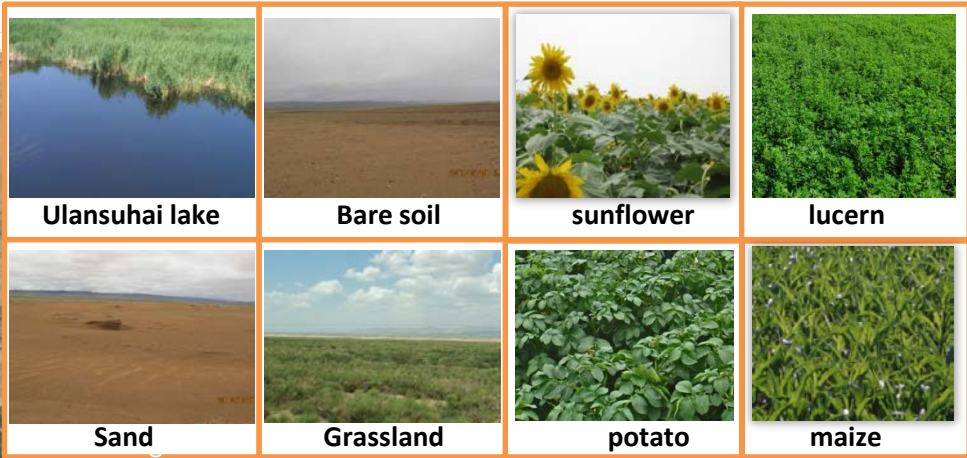
High-frequency automated radiometric calibration

- Located in Inner Mongolia, China, 50km away from Baotou city.
- A flat area of approximately 300km², about 1270m above sea level.
- Land cover: Sand, bare soil, grass, lake, various agriculture (maize, sunflower, lucern, potato, etc.).
- Features a cold semi-arid climate with approximately 300 clear-sky days per year.

Site overview:



Ulansu Lake



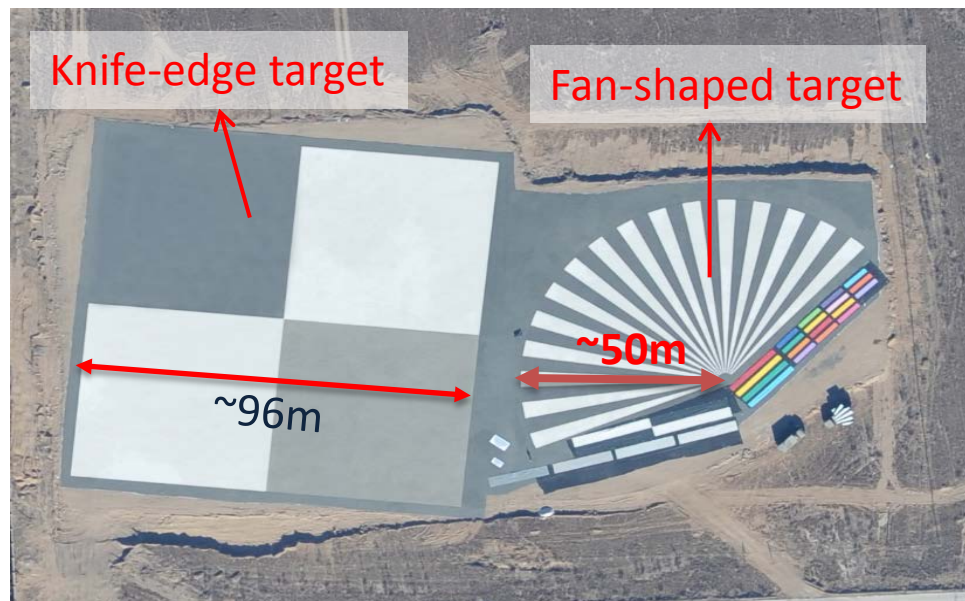
➤ 1. High-stable ground standard targets

1.1 Artificial Permanent Targets

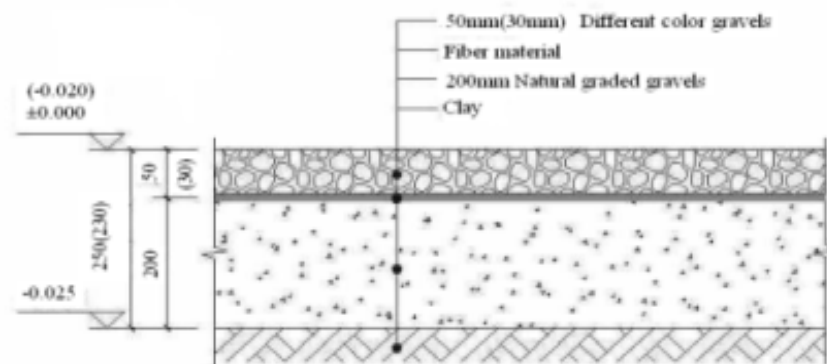
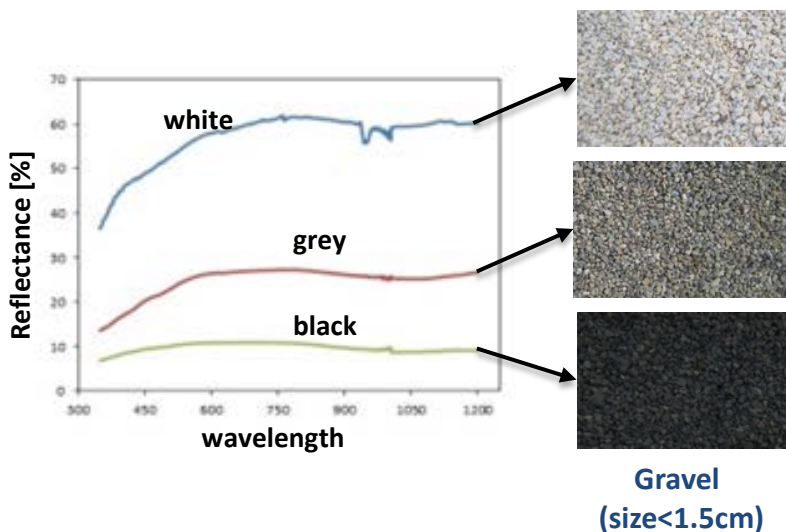
Optical edge and fan-shape target

Dedicated to high-accuracy and high-stable radiometric calibration:

- **High-stable**: made of natural gravels
- **Wide-range**: three grey-scale
- **Well-uniform**: each block filled with the same gravels



Aerial image of the optical artificial permanent targets

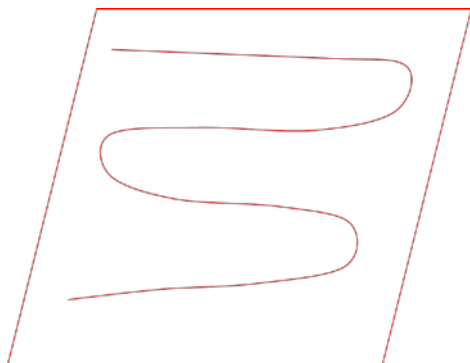




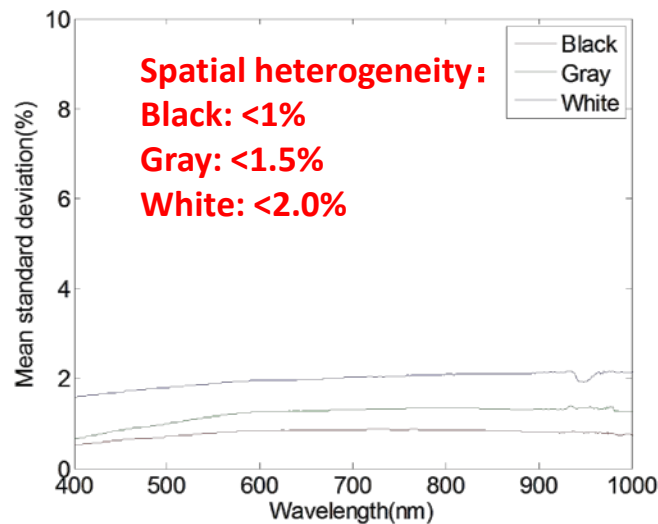
➤ 1. High-stable ground standard targets

1.1 Artificial Permanent Targets

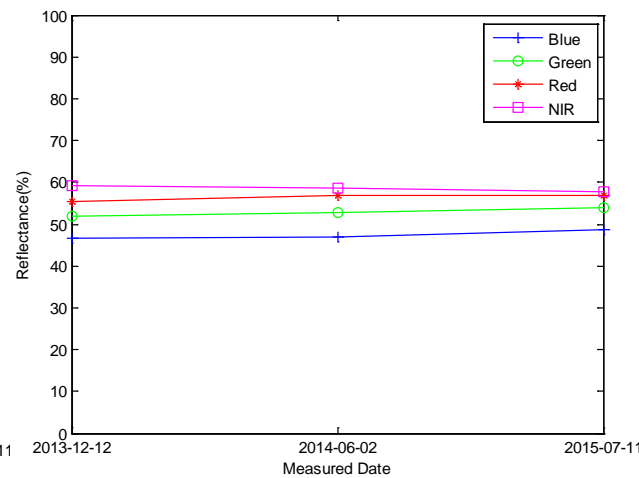
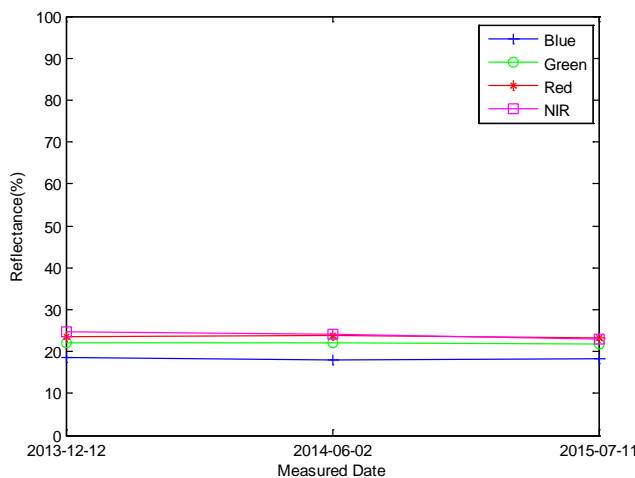
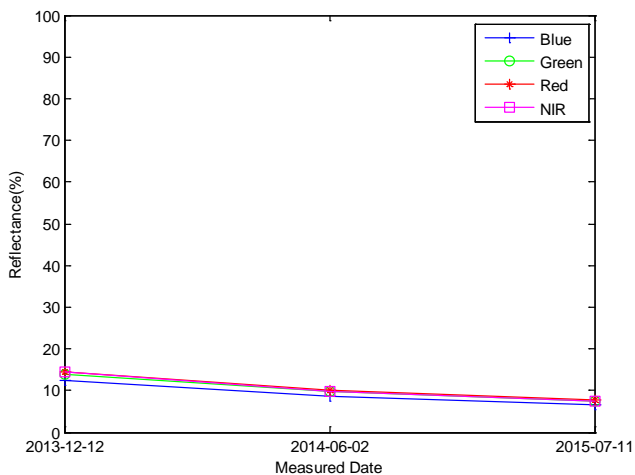
Uniformity of the edge target



Sampling strategy of the measurement



Annual degradation of the reflectance of three kinds of gravels



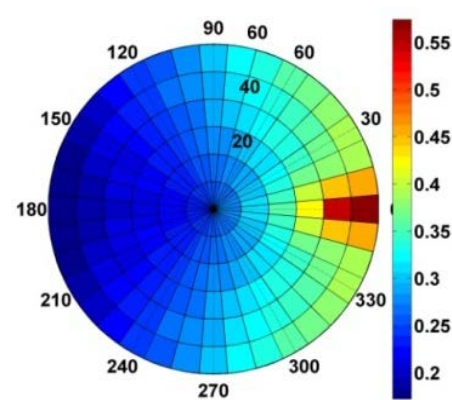
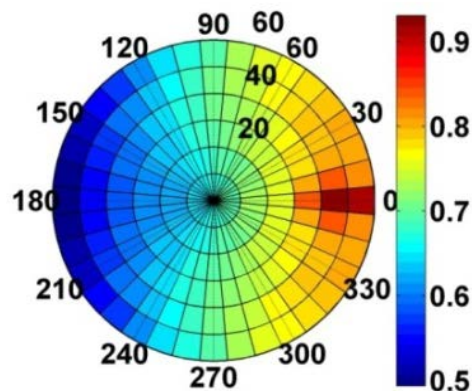
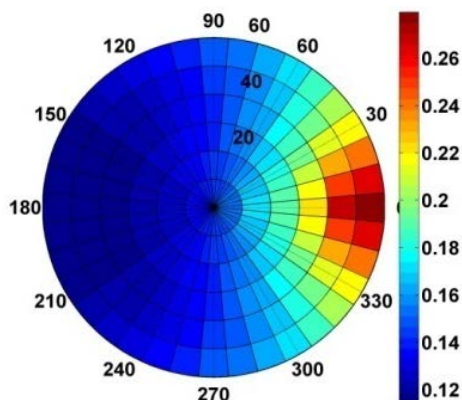
➤ 1. High-stable ground standard targets

1.1 Artificial Permanent Targets

In situ BRF measurement and modeling

- The relative difference of measured angular reflectance in three targets: <10% (VZA within $\pm 10^\circ$).
- The RMSE of BRDF model: <3% for three targets.

$$R(\theta_i, \theta_v, \phi, \lambda) = f_{iso}(\lambda) + f_{vol}(\lambda)K_{vol}(\theta_i, \theta_v, \phi, \lambda) + f_{geo}(\lambda)K_{geo}(\theta_i, \theta_v, \phi, \lambda)$$

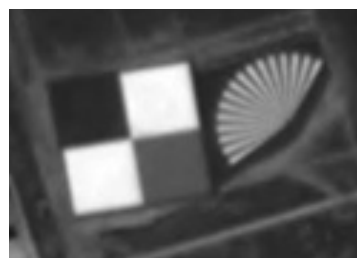
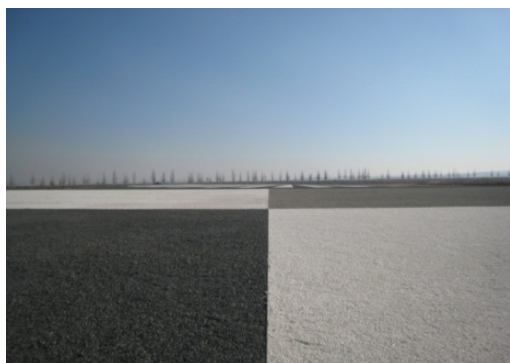


➤ 1. High-stable ground standard targets

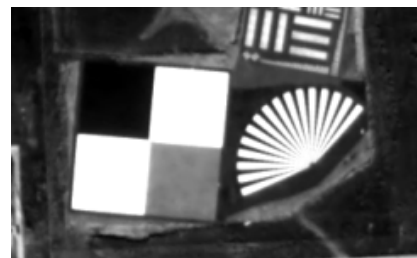
1.1 Artificial Permanent Targets

Optical edge and fan-shape target

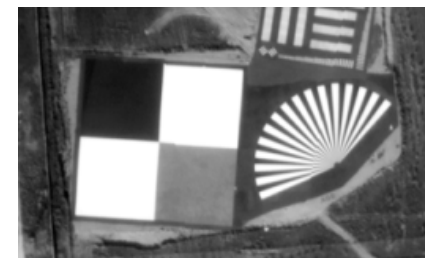
The construction of these targets was finished at the end of October, 2013. During the operation phase, the performance of several optical sensors were assessed.



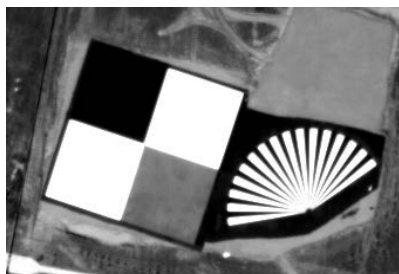
2013/11/4 GF-1 PAN image



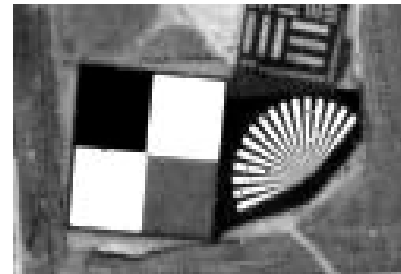
2014/10/13 GF-2 PAN image



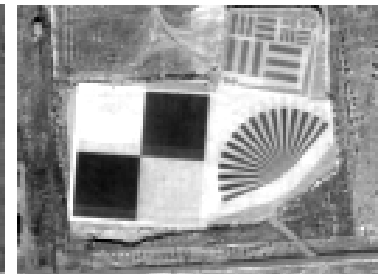
2014/11/29 KZ PAN image



2014/08/14 KOMPSAT-3 PAN image



2014/10/17 airborne SWIR sensor image



2014/10/17 airborne MIR sensor image

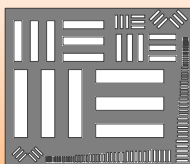


➤ 1. High-stable ground standard targets

1.1 Artificial Permanent Targets

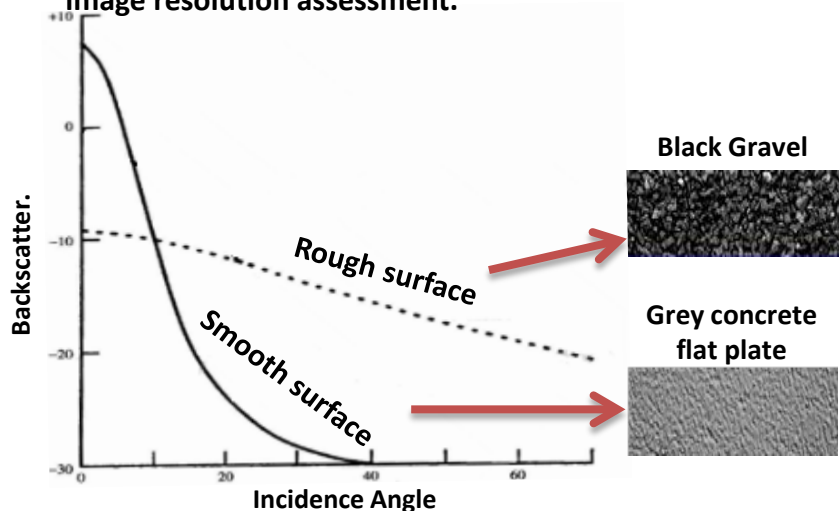
Microwave/optical bar-pattern target

1. "bar-pattern" design, rather than "point", benefiting for microwave image resolution assessment



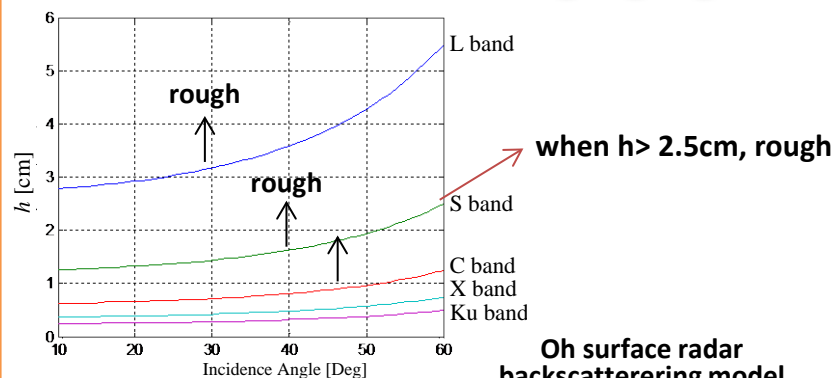
2. Intensity contrast between bars and the background is realized by their roughness difference

Black gravel and grey concrete flat plate were exploited to construct the target for both microwave and optical image resolution assessment.



3. The size of the gravel was calculated based on both Rayleigh roughness criterion and Oh surface radar backscattering model, in order to exhibit sufficient contrast in Ku to S band radar image.

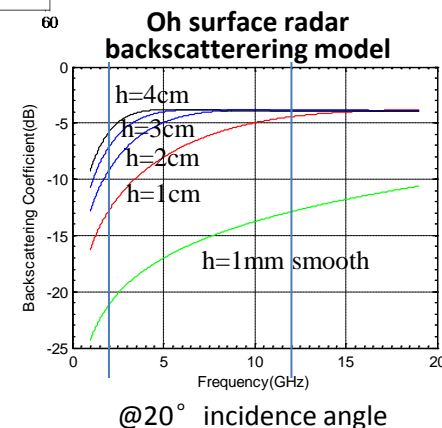
Rayleigh criterion: $h > \frac{\lambda}{8 \cdot \cos \theta}$



when $h=3\text{ cm}$,
contrast=12dB
at 5GHz

Gravel size $S=2h$:

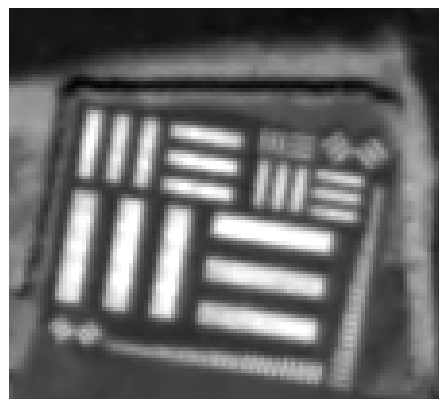
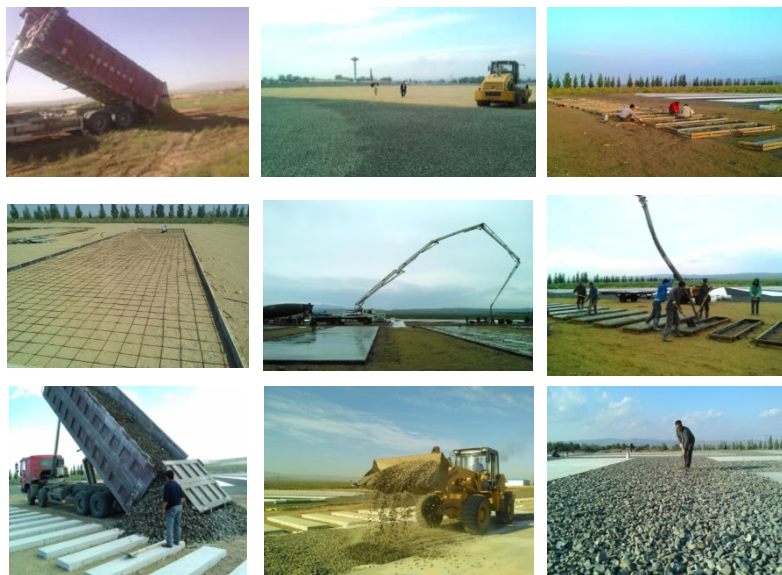
- <0.4m width bars:
 $S=2\text{cm} \pm 0.5$;
- >0.4m width bars:
 $S=5\text{cm} \pm 1$.



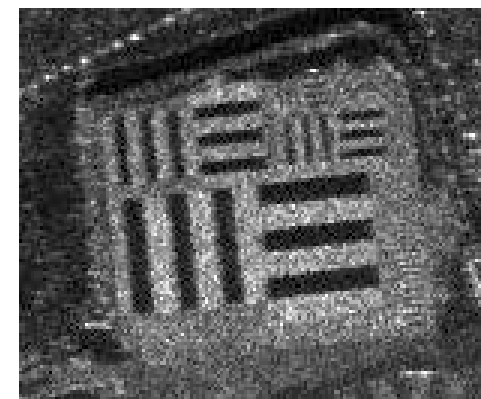
➤ 1. High-stable ground standard targets

1.1 Artificial Permanent Targets

Microwave/optical bar-pattern target



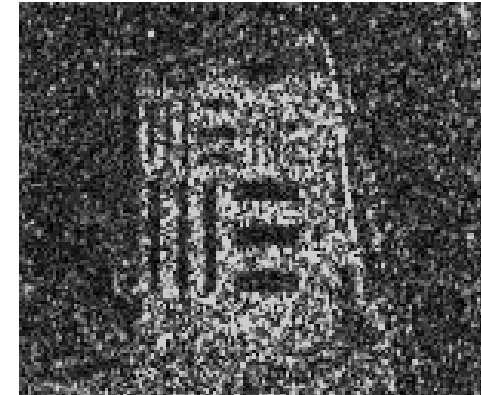
2014/10/13 GF-2 PAN image



2014/10/19 C-band airborne SAR image



2014/10/17 airborne SWIR image



2014/10/22 KOMPSAT-5 SAR image



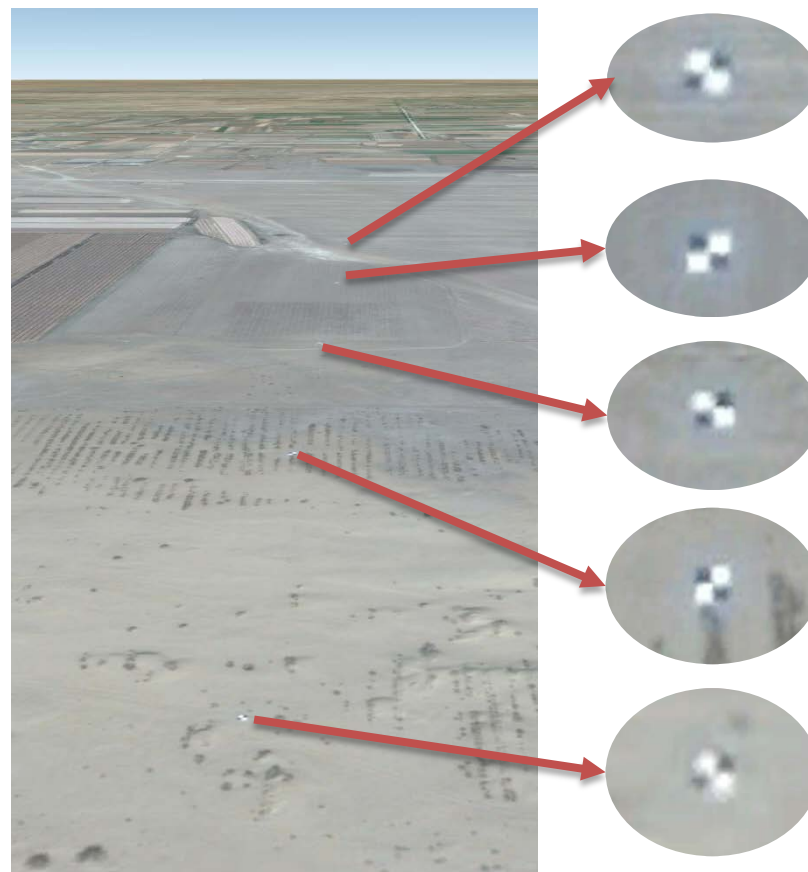
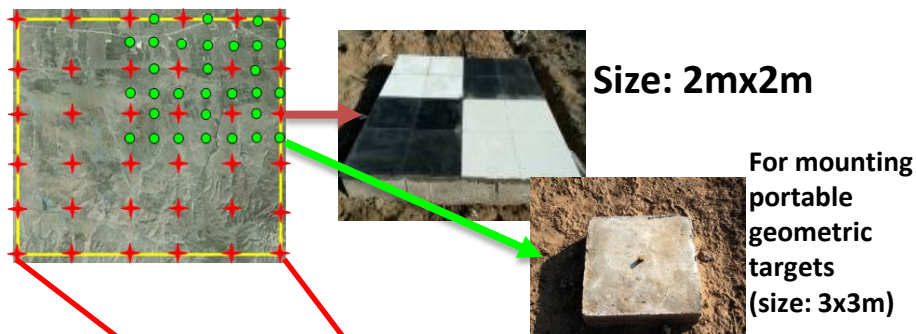
Finished construction by the end of September, 2014

➤ 1. High-stable ground standard targets

1.1 Artificial Permanent Targets

Geometric control points

75 geometric control points with positional accuracy of 2cm(horizontal), 4cm (vertical).



GCP Google Earth image(from Digital Global, 0.5m)

➤ 1. High-stable ground standard targets

1.1 Artificial Permanent Targets

SAR corner reflector base

Distribution direction (east-west) is 95° to North, with compromise of transportation convenience and SAR flight direction:

$$\beta = \arcsin \frac{\pm \cos \alpha}{\cos \xi} \approx 10^\circ$$

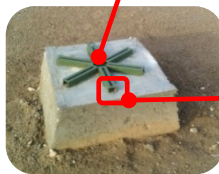
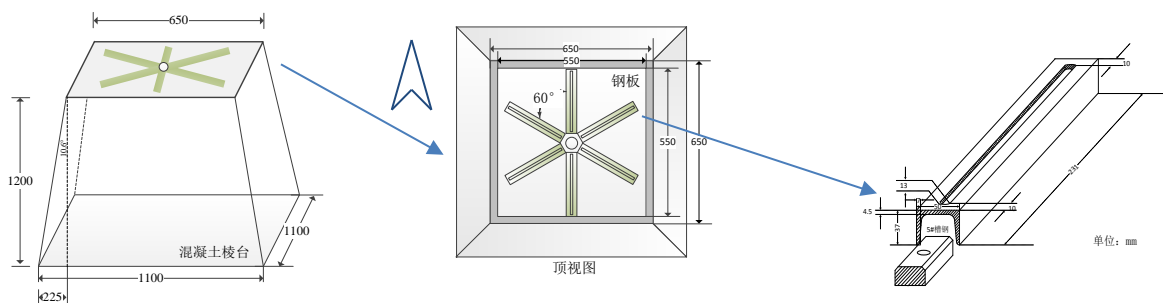
β : Azimuth

α : Latitude

ξ : Inclination

| Satellite | Inclination |
|------------|-------------|
| TerraSAR | 97.44° |
| Radarsat-2 | 98.6° |
| Sentinel-1 | 98.18° |
| SkyMed | 97.86° |
| HJ-1-C | 97.37° |

For quickly deploying corner reflectors and avoiding repeated measurement of position information



➤ 1. High-stable ground standard targets

1.2 Artificial Portable Targets

Optical



Knife-edge




Color targets



Fan-shaped



Array of point source targets







Grayscale





Low-emissivity Target(4mx4m)

Microwave

| Triangular Trihedral CRs | Hexagonal Trihedral CRs | Dihedral Trihedral CRs | Bottom-extended Trihedral CRs |
|--|--|---|--|
|  |  |  |  |

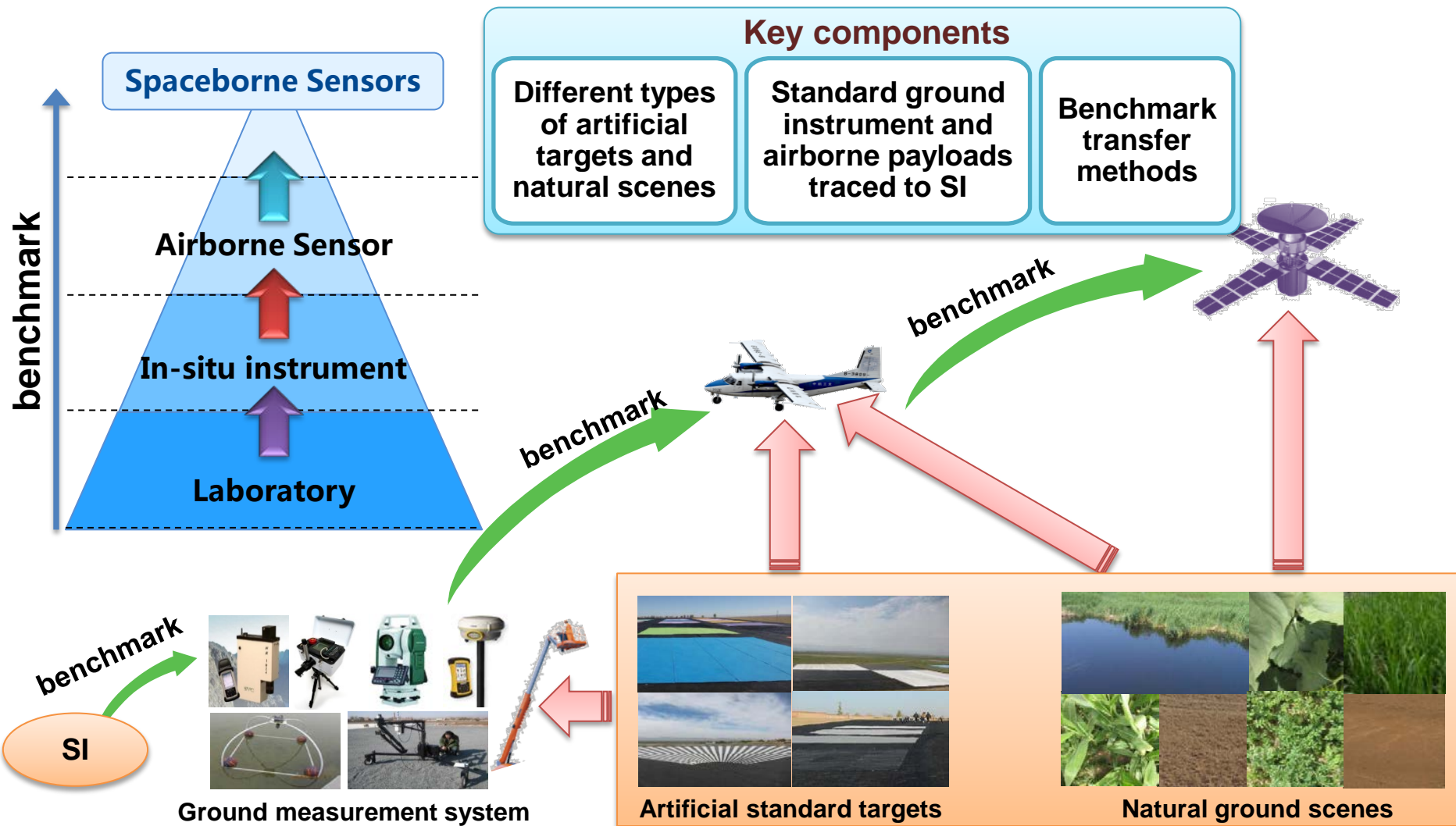
Square Trihedral CRs





➤ 2. High-accuracy Stepwise Cal&Val system

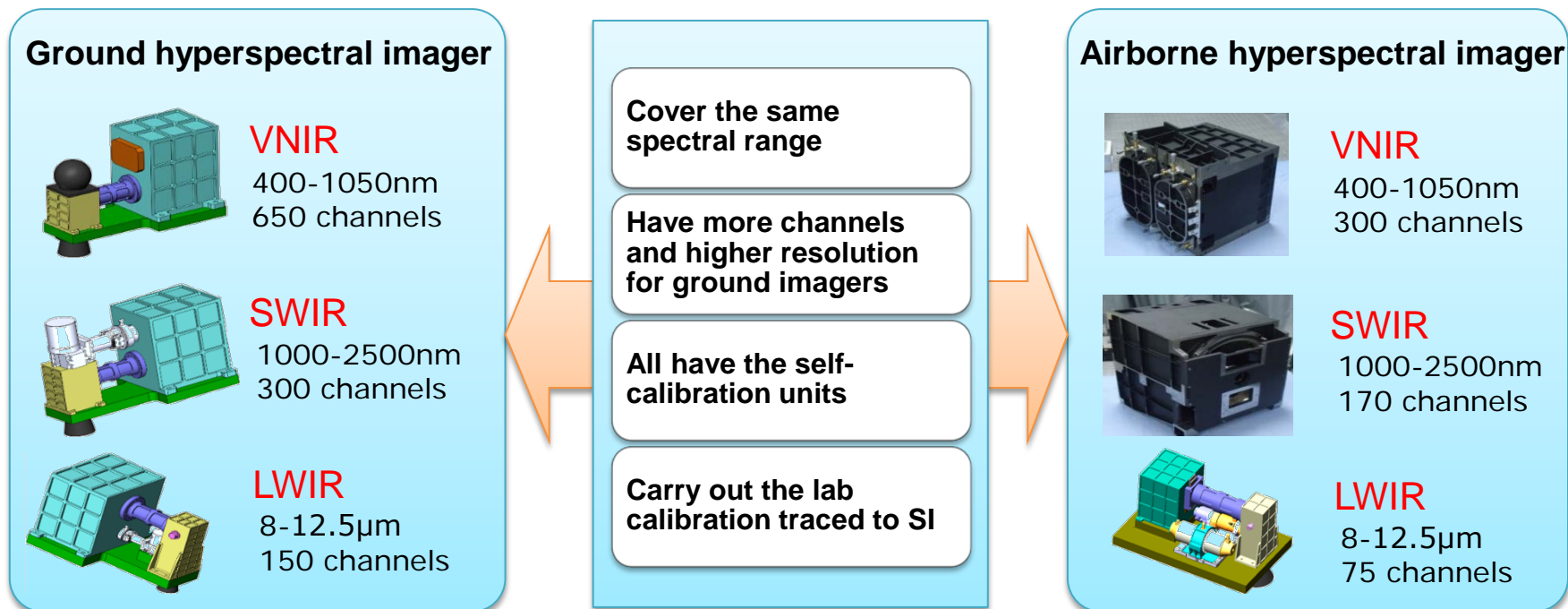
The system aims to develop a chain that transfers the benchmark from laboratory to spaceborne sensors.





➤ 2. High-accuracy Stepwise Cal&Val system

In order to obtain the “truth” of ground scenes and targets, the Stepwise Cal&Val system are integrated and some standard payloads are still under-development.



Total station and GPS



VIS-IR Field Spectrometers



LAI-2200C plant canopy analyzer



Overhead working platform



Photoelectric 19 stabilized platform



➤ 2. High-accuracy Stepwise Cal&Val system

Benchmark transfer methods:

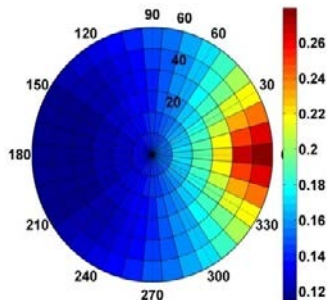
Angular Matching

Develop BRDF model for typical targets:

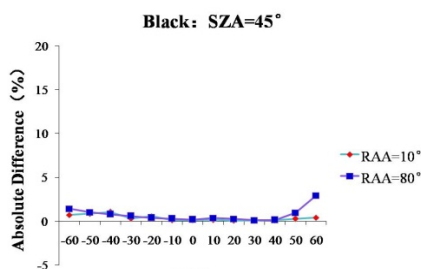
$$R(\theta_i, \theta_v, \phi, \lambda) = f_{iso}(\lambda) + f_{vol}(\lambda)K_{vol}(\theta_i, \theta_v, \phi, \lambda) + f_{geo}(\lambda)K_{geo}(\theta_i, \theta_v, \phi, \lambda)$$



Target
(black gravels)



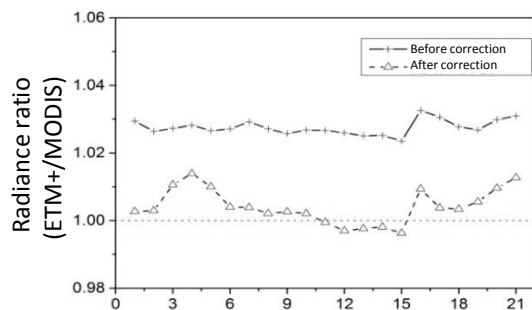
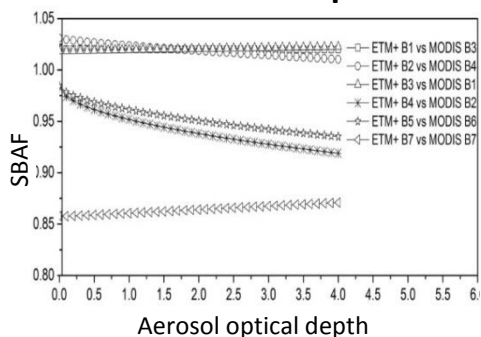
Modeled BRFs



Modeling
absolute differences

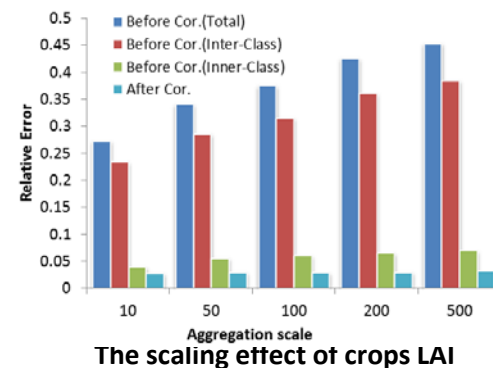
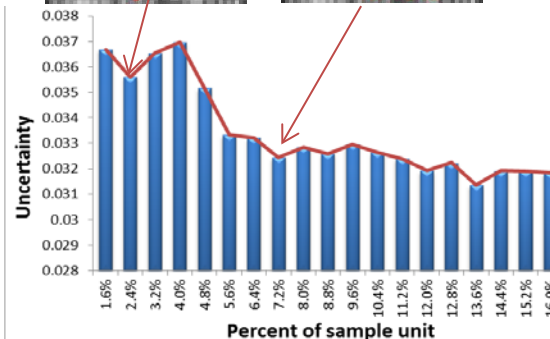
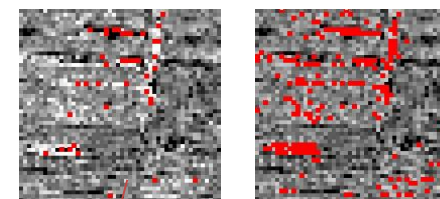
Spectral Matching

Improve the spectral band adjustment factor (SBAF) by taking into account for the atmospheric effects



Spatial Transformation

The optimal sampling strategy considering the cost-effectiveness





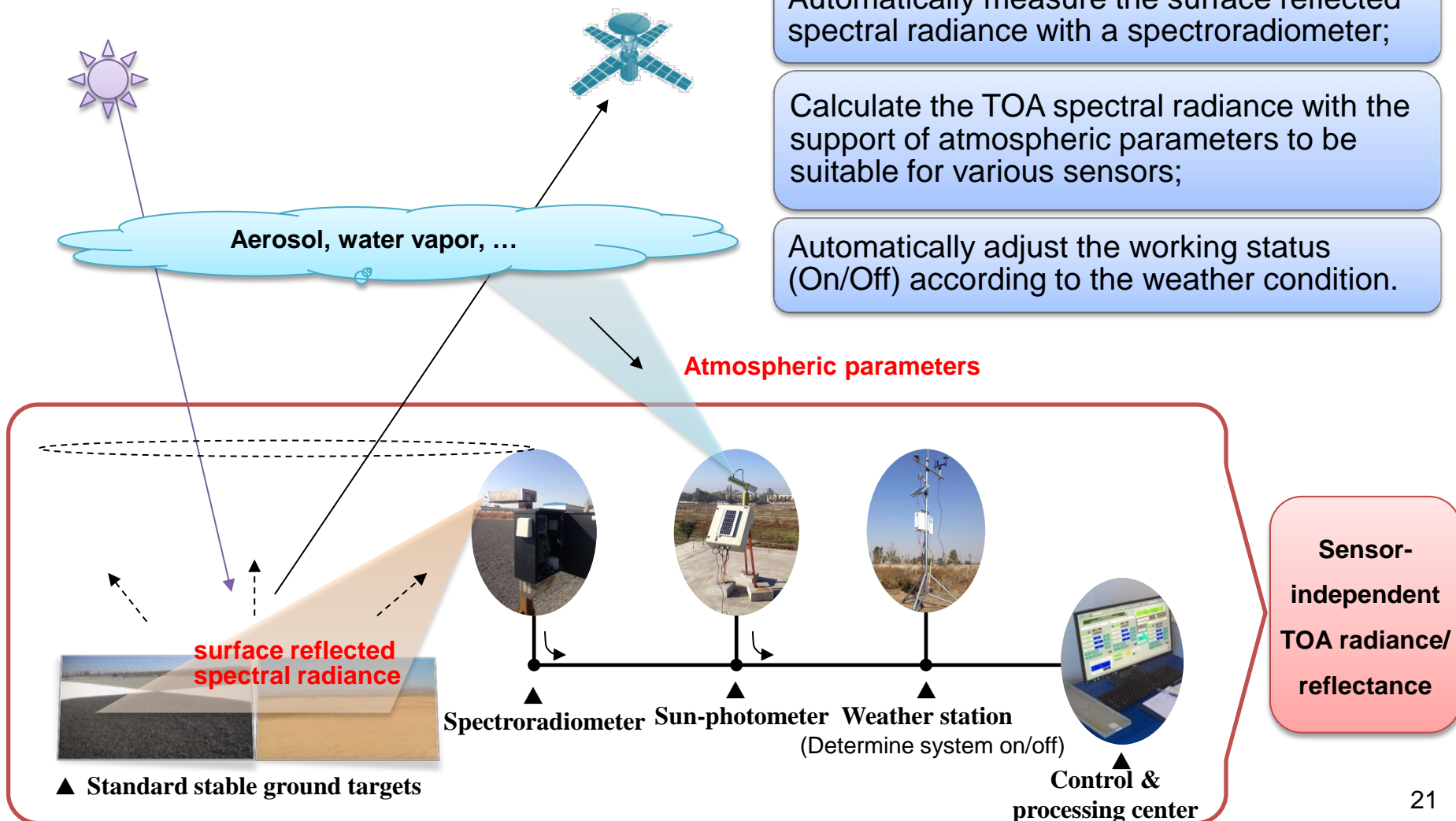
➤ 3. High-frequency automated radiometric calibration

Automated reflectance spectrum measurement system

Automatically measure the surface reflected spectral radiance with a spectroradiometer;

Calculate the TOA spectral radiance with the support of atmospheric parameters to be suitable for various sensors;

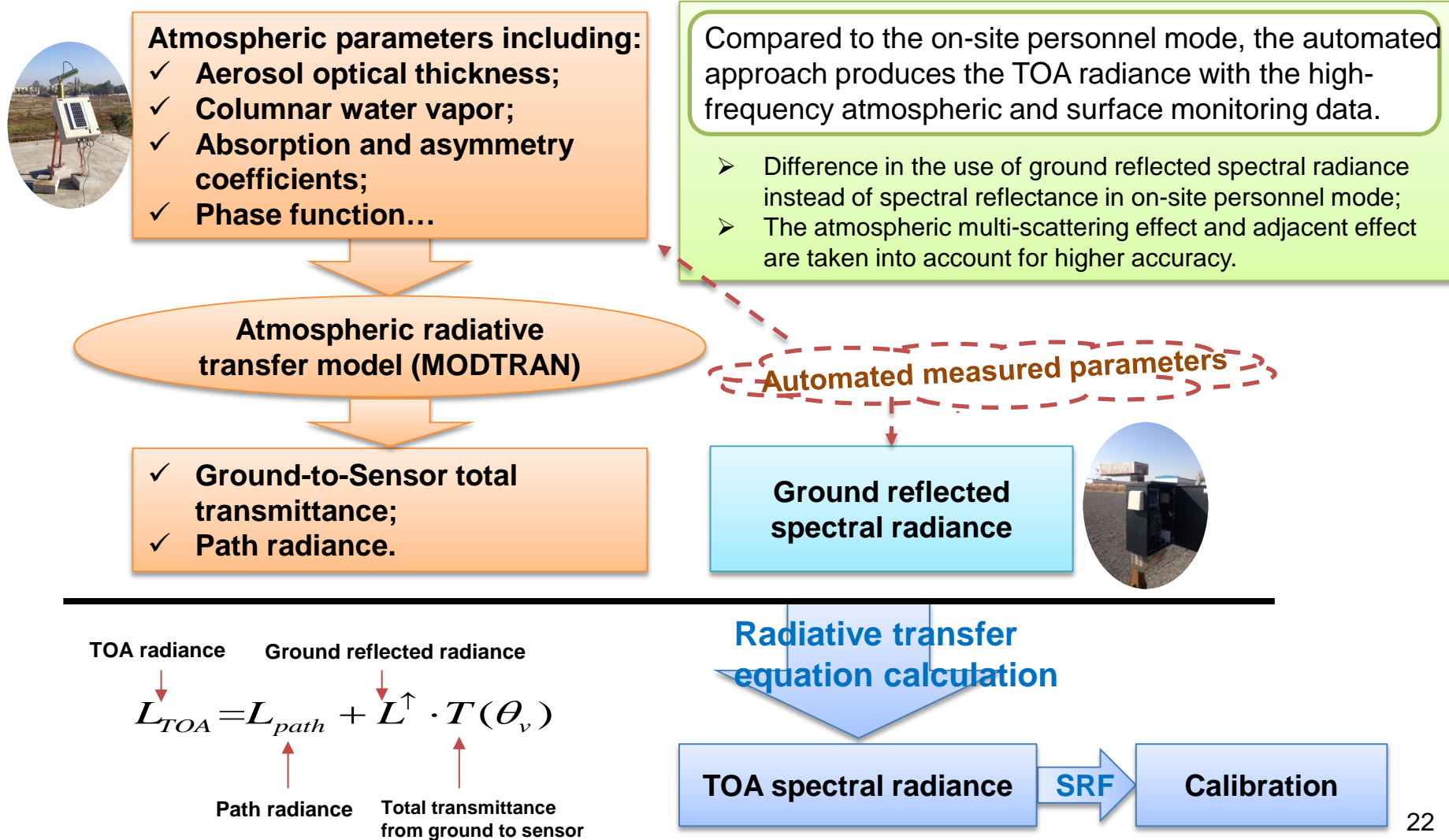
Automatically adjust the working status (On/Off) according to the weather condition.

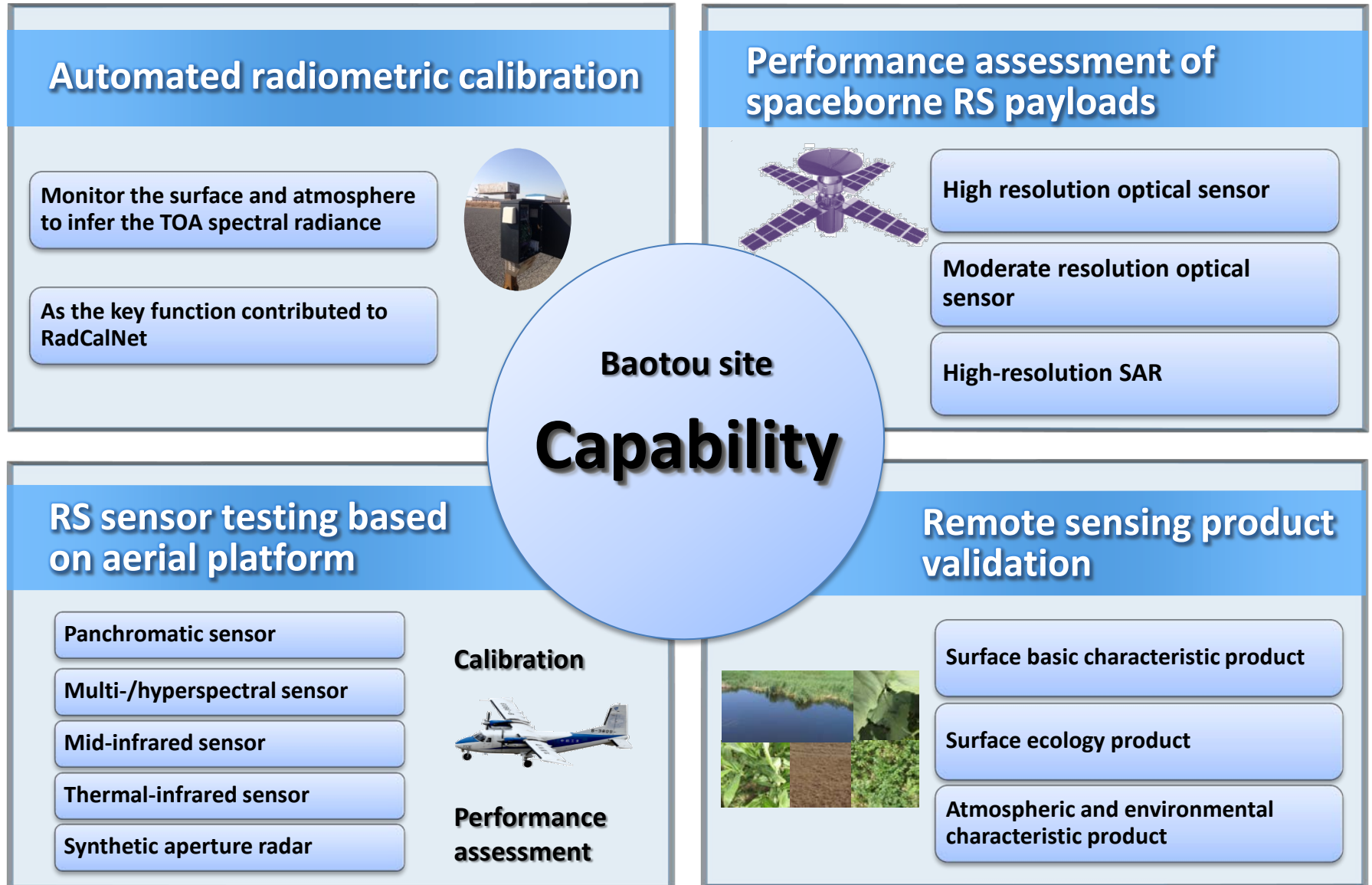




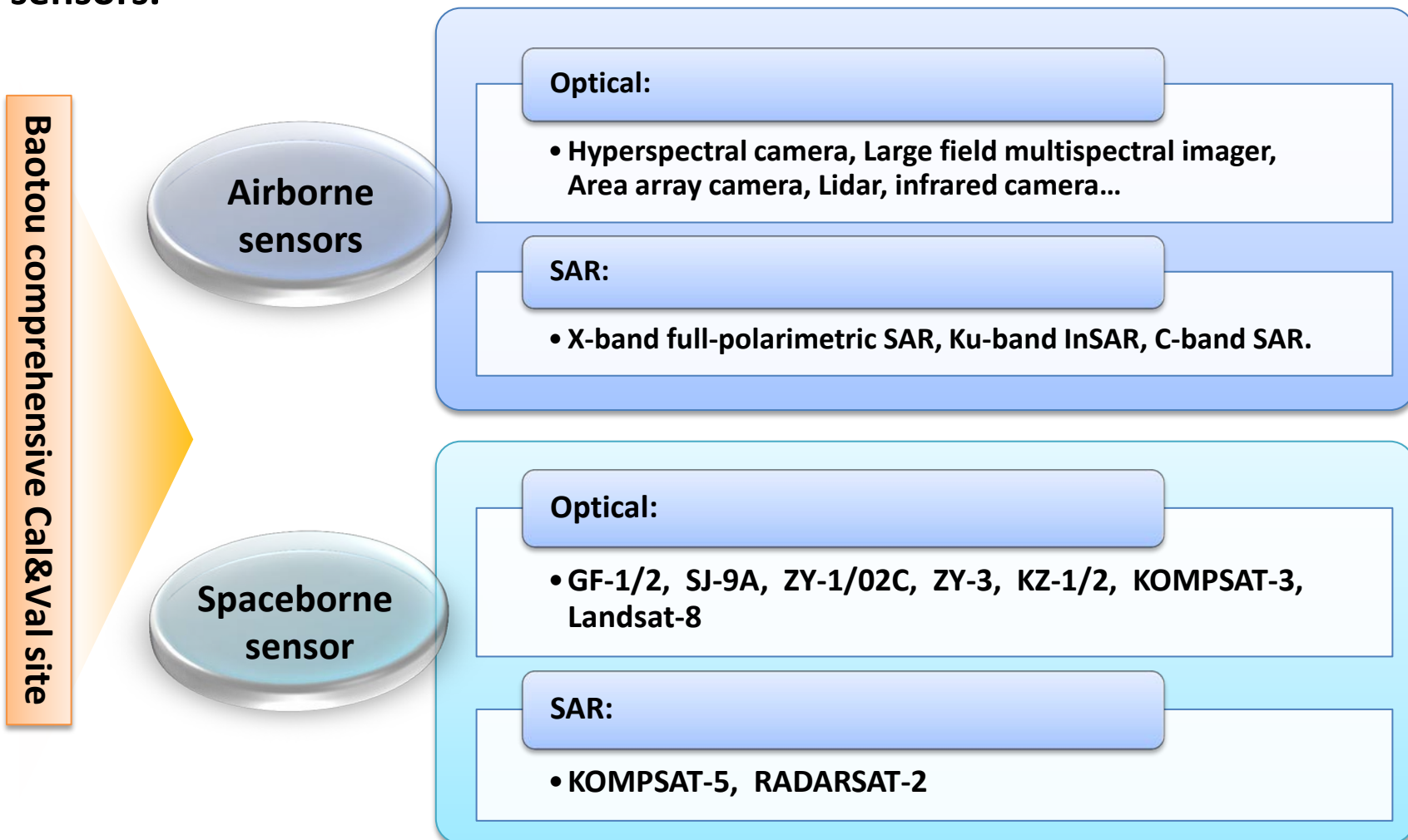
➤ 3. High-frequency automated radiometric calibration

Automated measurement processing procedure





During 2009 to 2015, multiple scientific flight campaigns were carried out in Baotou site, including more than 11 airborne sensors and 12 spaceborne sensors.

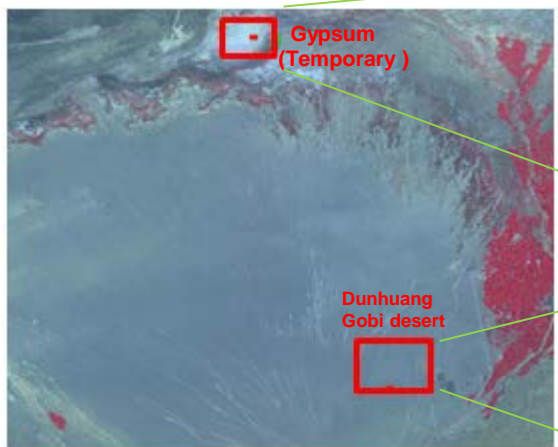




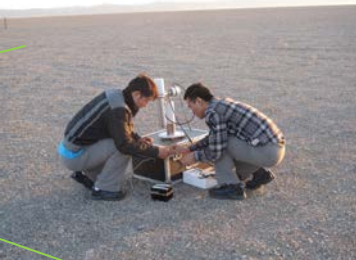
➤ Case1. Radiometric calibration in simultaneous mode

In China, the traditional vicarious calibration method for optical sensors mainly depend on Dunhuang site (Gobi). In recent years, some temporary fields with different reflectance were added to perform wide-range calibration.

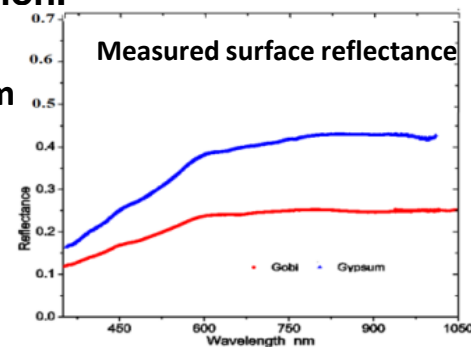
But the surface uniformity and stability of these fields are not ideal, and can not be covered within a single image.



Site1:Gypsum

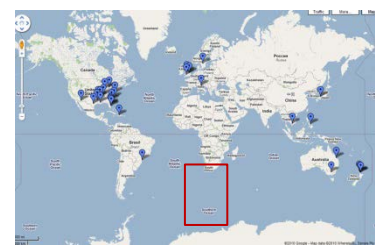


Site2:Dunhuang Gobi desert

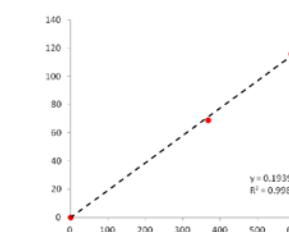
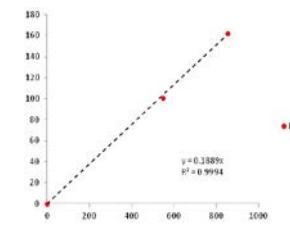
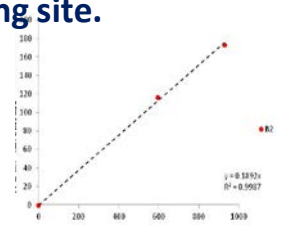
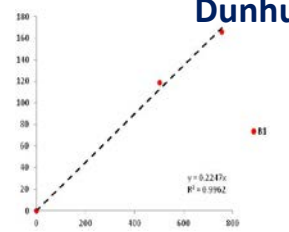
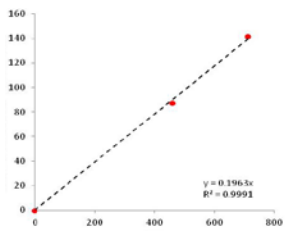


GF-1 calibration over Dunhuang site (Aug, 2014)

The sun photometer was installed temporarily on Dunhuang site.



Site3: Deep sea

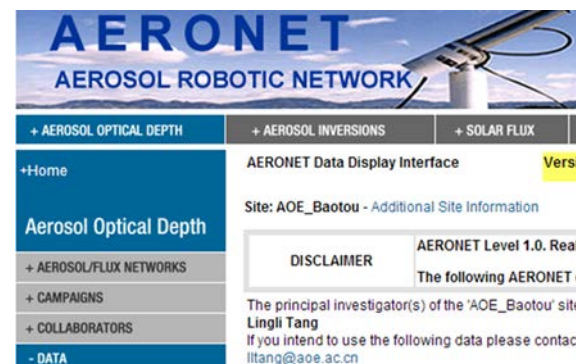
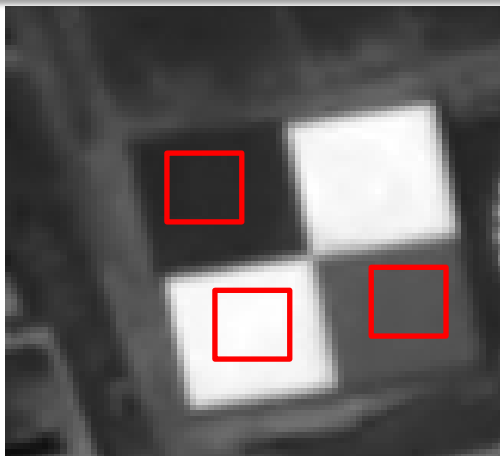




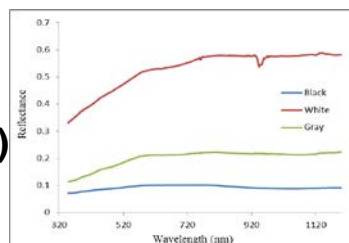
➤ Case1. Radiometric calibration in simultaneous mode

Baotou site has been greatly improved in a wide dynamic, stable, uniform ground standard targets for calibration. In addition, the sun photometer in this site joined the AERONET, providing quality-assured atmospheric data.

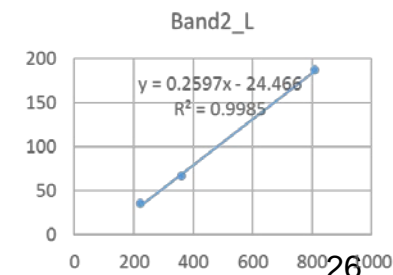
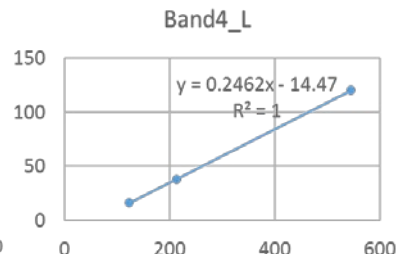
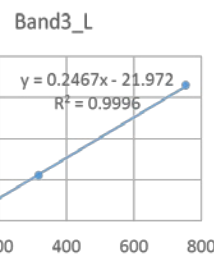
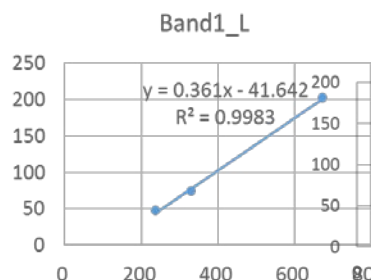
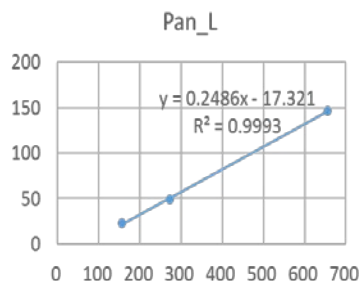
Case for the vicarious calibration of GF-1



GF-1 image over Baotou site(2014-10-13)



Reflectance

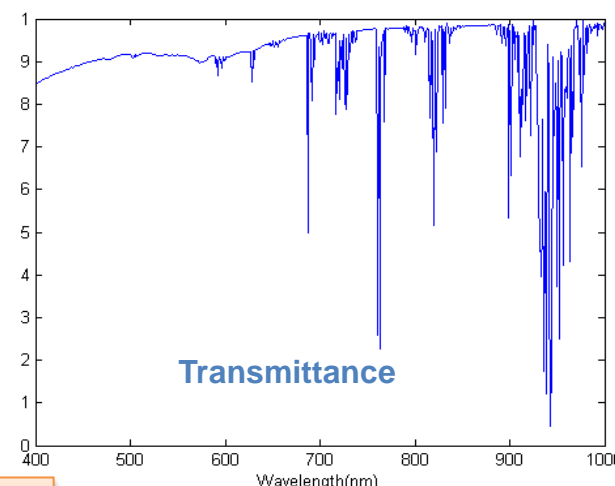
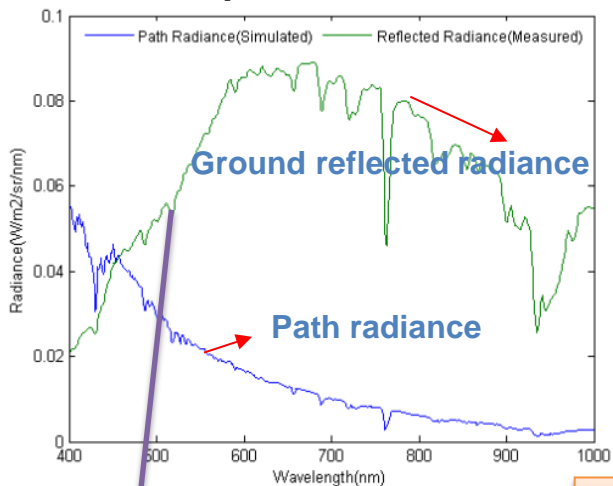


➤ Case2. Radiometric calibration in automated mode

Case study: Simulation of TOA radiance for OLI/Landsat 8

- 1. Calculation of atmospheric radiative transfer and TOA spectral radiance

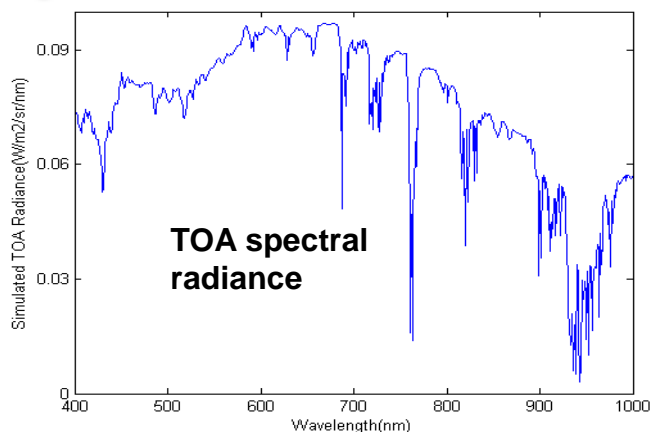
Data acquisition time : March 27, 2015



Total transmittance and path radiance were simulated with the automated atmospheric observations.



The ground reflected radiance was measured at the sand field in Baotou site.

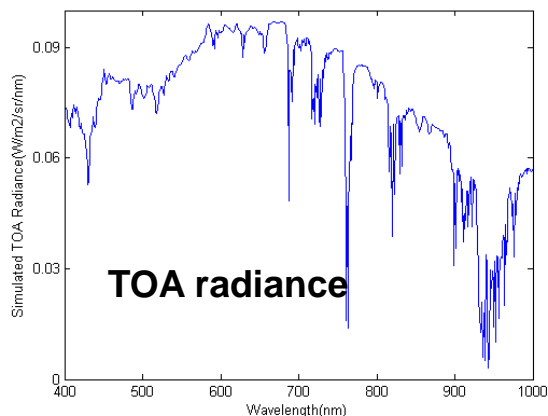


TOA spectral radiance was calculated based on the RTE.

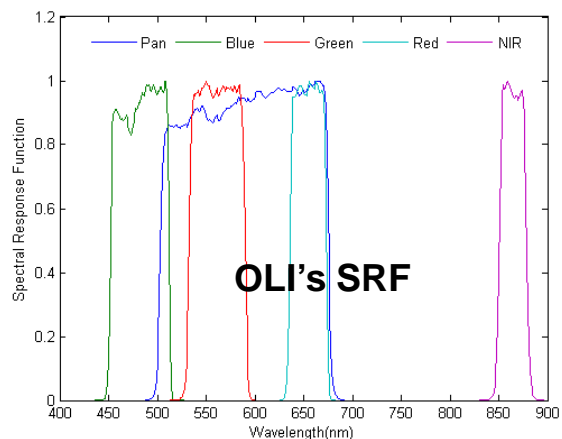


➤ Case2. Radiometric calibration in automated mode

• 2. Prediction of channel TOA radiance and inter-comparison



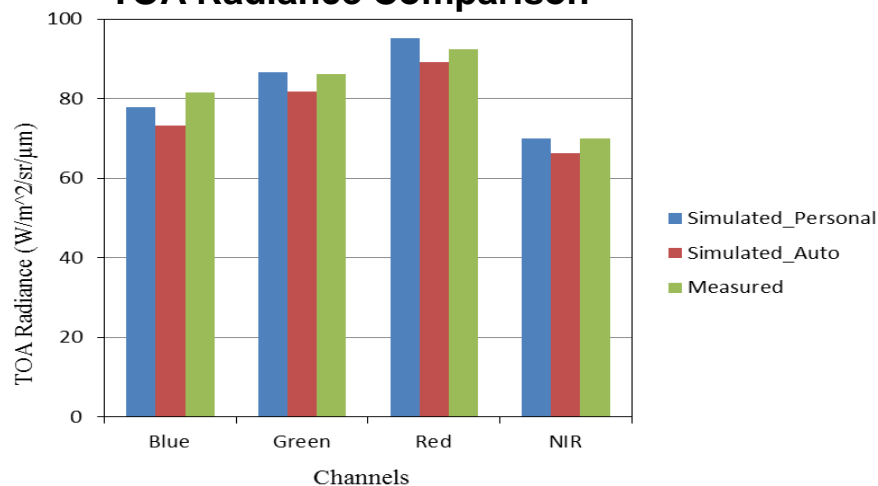
+



Convolution

| | Observed Rad. | Simulated Rad. | | | |
|--------------|---------------|----------------|--------------|------------------------|--------------|
| | | Automated mode | | On-site personnel mode | |
| | Value | Value | RE | Value | RE |
| Blue | 81.59 | 73.19 | 10.2% | 77.90 | 4.5% |
| Green | 86.11 | 81.74 | 5.0% | 86.71 | 0.7% |
| Red | 92.38 | 89.13 | 3.5% | 95.09 | 2.9% |
| NIR | 70.10 | 66.25 | 5.4% | 70.05 | 0.06% |

TOA Radiance Comparison



The relative difference for automatic mode is higher than on-site personnel mode. More detailed analysis will be performed to improve the automatic calibration approach.

➤ Case1. Radiometric calibration in an automated mode

• 3. Uncertainty analysis of automated radiometric calibration

The calculation equations of automated radiometric calibration

$$L_{TOA} = L_g \cdot \tau + L_p$$



The sources of uncertainty

- The instrument: calibration errors, repeatability of radiospectrometer
- The target: uniformity, BRDF
- The atmosphere: aerosol optical depth, water vapour, aerosol type, ozone, etc...
- The model: accuracy of MODTRAN, solar irradiance, etc...
- Others: observation time, cloud, etc...

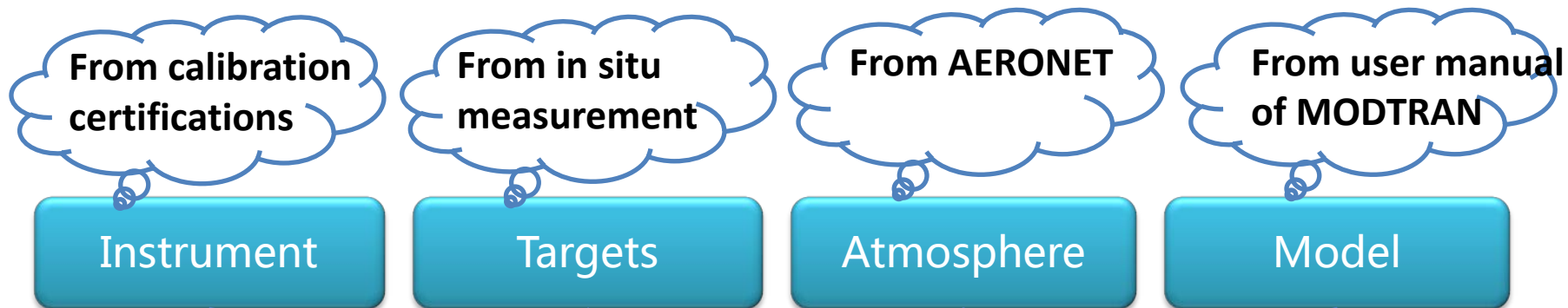


The measurement equation

$$L_{TOA} = [(L_g \cdot K_{cal} \cdot K_{rep} \cdot K_{uni} \cdot K_{BRDF}) \cdot (\tau \cdot K_{AOD} \cdot K_{ars_m} \cdot K_{CWV} \cdot K_{atp} \cdot K_{MODTRAN}) + (L_p \cdot K'_{AOD} \cdot K'_{ars_m} \cdot K'_{CWV} \cdot K'_{atp} \cdot K'_{MODTRAN} \cdot K_{sol_ir})] \cdot K_{model} \cdot K_t$$

➤ Case1. Radiometric calibration in an automated mode

• 3. Uncertainty analysis of automated radiometric calibration



$$L_{TOA} = L_g \cdot \tau + L_p$$

Changing the value of one of the factors to find how the TOA radiance will be changed, and to calculate the uncertainty associated with TOA radiance due to this factor. Then, the total uncertainty is calculated according to the law of propagation of uncertainties.

$$u_c^2(y) = \sum_{i=1}^n \left(\frac{\partial f}{\partial x_i} \right)^2 u^2(x_i) + 2 \sum_{i=1}^{n-1} \sum_{j=i+1}^n \frac{\partial f}{\partial x_i} \frac{\partial f}{\partial x_j} u(x_i, x_j)$$



➤ Case1. Radiometric calibration in an automated mode

• 3. Uncertainty analysis of automated radiometric calibration

Uncertainty budget

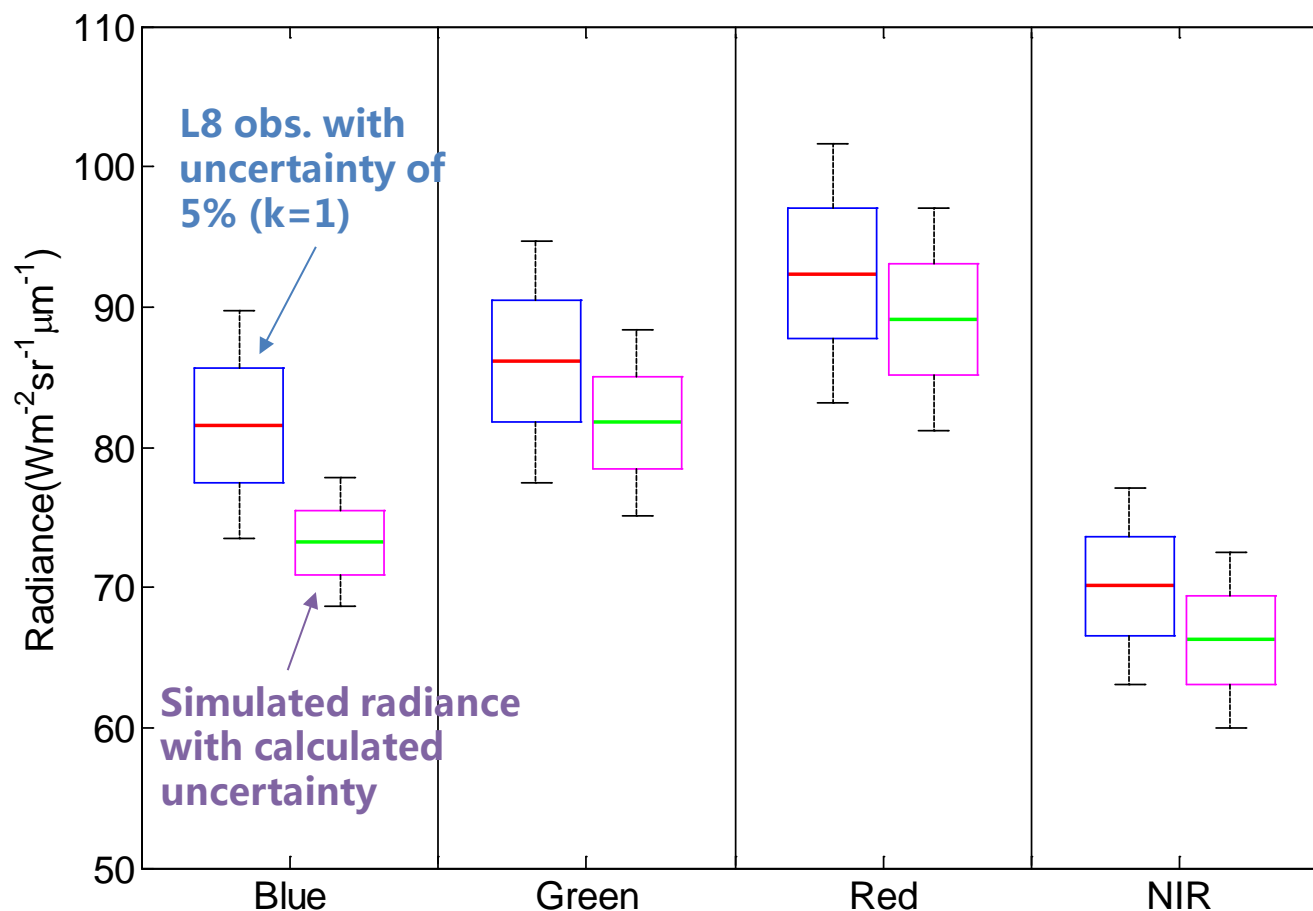
| Uncertainty component | | Associated uncertainty | | Sensitivity coefficient | Uncertainty associated with L_{toa} due to this | | | |
|--------------------------|------------------|-------------------------|-----------------|-------------------------|---|---------------|---------------|---------------|
| | | absolute | relative | | Blue | Green | Red | NIR |
| Instrument | Calibration | --- | 4% | 1 | 2.415% | 3.304% | 3.683% | 3.894% |
| | Repeatability | --- | | 1 | 0.017% | 0.015% | 0.013% | 0.033% |
| Target | Uniformity | --- | 2.17% | 1 | 1.310% | 1.793% | 1.998% | 2.112% |
| | BRDF | --- | ~1.5% | 1 | 0.905% | 1.239% | 1.381% | 1.460% |
| Atmospheric | AOD | --- | 5.5% | 1 | 0.113% | 0.055% | 0.023% | 0.004% |
| | CWV | --- | 10% | 1 | 0.005% | 0.011% | 0.018% | 0.004% |
| | Solar irradiance | --- | 1% | 1 | 0.396% | 0.174% | 0.079% | 0.027% |
| Model | MODTRAN | Transmittance ±0.005 | Radiance ±2% | 1 | 1.122% | 0.804% | 0.646% | 0.548% |
| | Simplified RTE | --- | | 1 | 0.022% | 0.067% | 0.113% | 0.011% |
| Total uncertainty | | | | | 3.130% | 4.044% | 4.461% | 4.696% |

➤ Case1. Radiometric calibration in an automated mode

• 3. Uncertainty analysis of automated radiometric calibration

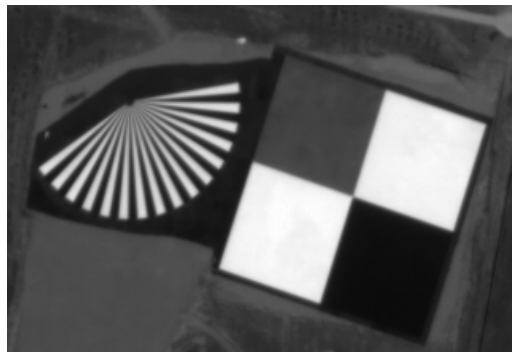
The calculated radiance is consistent with Landsat 8 observations, but more bias can be found in blue band.

More comparison results are needed to achieve reliable conclusion.

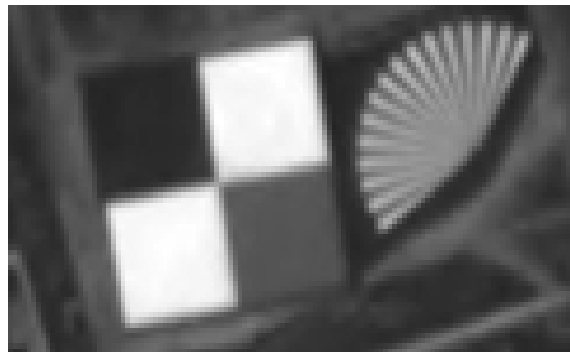


➤ Case 3. Performance assessment for high-resolution optical sensors

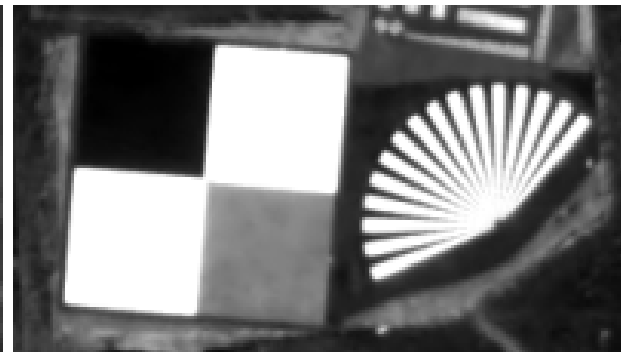
- **MTF**



KOMPSAT-3 panchromatic image



GF-1 panchromatic image
View zenith angle: 1.7°



GF-2 panchromatic image
View zenith angle: 8.86°

| KOMPSAT (2014/8/14) | AOE's results | KARI's results |
|------------------------|------------------|-------------------|
| Along track | 0.083 | 0.091 |
| Cross track | 0.105 | 0.106 |

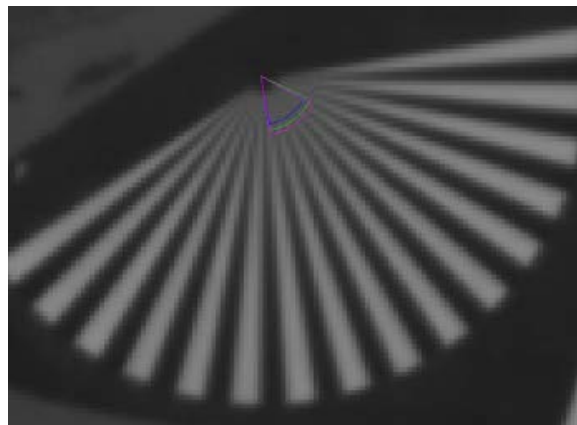
| | GF-1 (2013/11/4) | GF-2 (2014/ 10/13) |
|-------------|---------------------|-----------------------|
| Along track | 0.0217 | 0.0722 |
| Cross track | 0.0467 | 0.0933 |

An improved “knife-edge” method was used, which has three aspects of improvements on the ISO 12233 method :

- The use of the Fermi function for edge detection.
- Filter the ESF curves using S-G filter for noise suppression.
- Process LSF curve with Hamming window for avoiding spectral leakage and making more LSF central symmetry.

➤ Case 3. Performance assessment for high-resolution optical sensors

• Spatial resolution

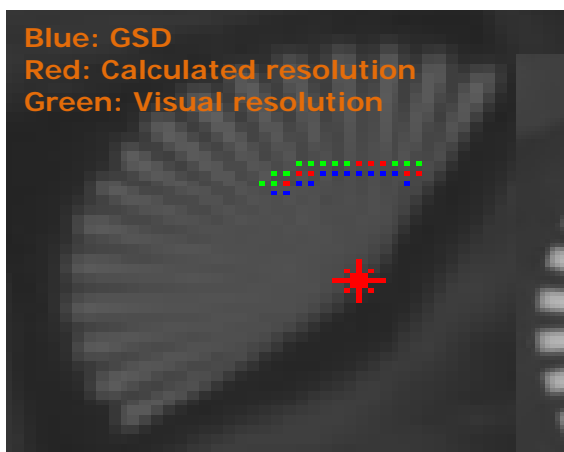


KOMPSAT-3 panchromatic image
on August 14, 2014

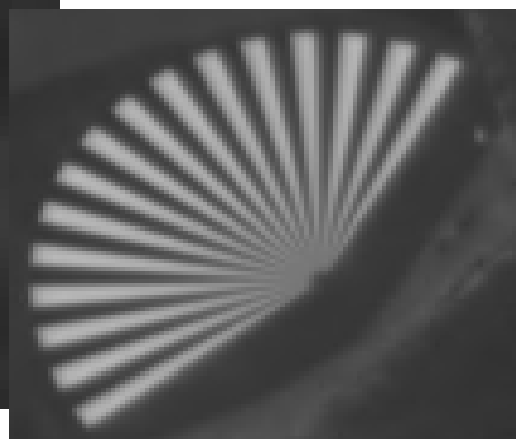
Automated detection algorithm for calculating resolution:

- Take the maximum radius of the target as a reference radius r_2 .
- Select an area containing 5 white segments .
- Detect the number of white segment for a certain radius $r < r_2$ when DN differences between white and black segment < 5 , and the limited radius r_0 is acquire when number of white segment < 4 .
- Calculated resolution = $r_0 * \phi$ (where ϕ is the angle of each segment).

| | KOMPSAT-3(2014/8/14) |
|-----------------------|----------------------|
| GSD | 0.7m |
| Calculated resolution | 0.79m |
| Visual resolution | 0.73m |



GF-1 panchromatic image
View zenith angle: 1.7°

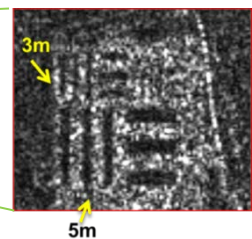
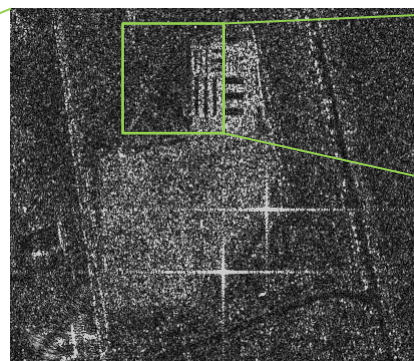


GF-2 panchromatic image
View zenith angle: 8.86°

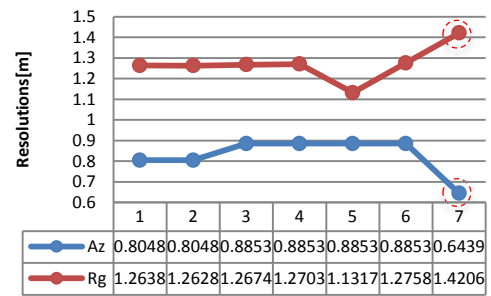
| | GF-1 (2013/11/4) | GF-2 (2014/10/13) |
|-----------------------|---------------------|----------------------|
| GSD | 2m | 1m |
| Calculated resolution | 2.16 m | 1.13m |
| Visual resolution | 2.22m | 1.05m |

➤ Case 4. Image quality assessment for KOMPSAT-5 SAR

KOMPSAT-5 SAR image on October 22, 2014(HH)



The "image resolution" is better than 3m.

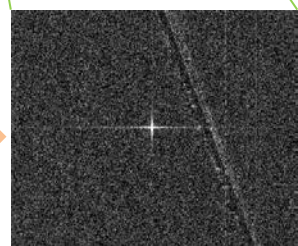


- Nominal resolution:
- Ground range instrument geometric resolution: 1.21m
 - Azimuth instrument geometric resolution: 0.90m

The resolution assessment results of the seven CRs are consist with each other except CR#7. The image of CR#7 is not a ideal point response image.

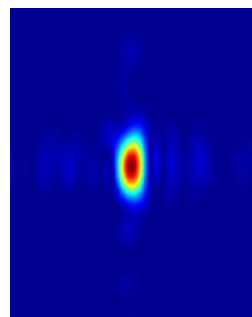


Corner reflector

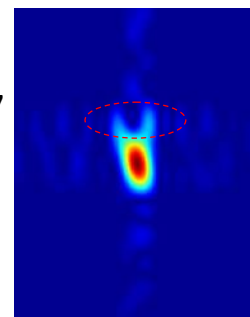


SAR image

CR #1

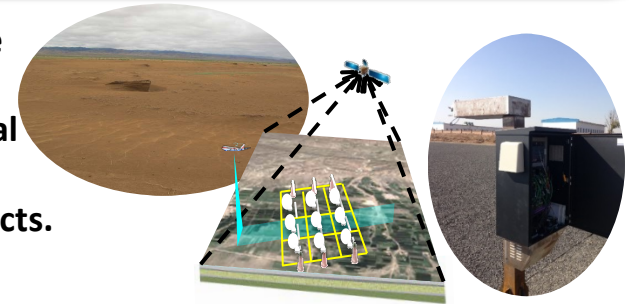


CR #7



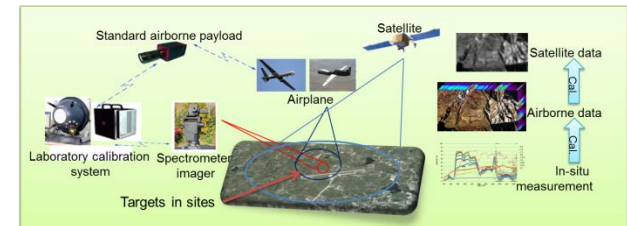
1. Strengthen the capability to support long-term calibration operation

- Improve auto-observation/calibration system to provide precise Cal&Val service in an operational way.
- Introduce more large-area natural scenes to improve the Cal&Val function for the moderate/coarse resolution sensors.
- Expand the functions on the validation of remote sensing products.



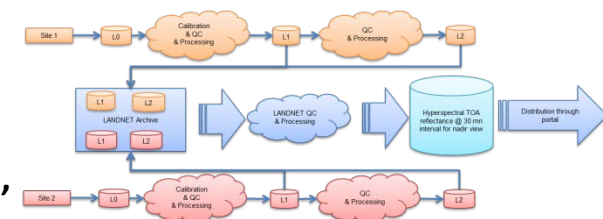
2. Upgrade consistent traceable approach for quality control

- Complete the development of VNIR, SWIR and TIR hyperspectral imagers.
- Study on the temporal, spatial, spectral and viewing angle matching technologies, decreasing significant scaling bias.
- Characterize the uncertainties and perform quality controlling in the whole benchmark transfer chain.



3. Offer contribution to the “global calibration” of EO through RADCALNET

- Participate the RADCALNET activities, including the inter-calibration of the instrument, technique support for making guidelines or standards, and collaboration with other networks, so as to demonstrate the feasibility of the concept for “global calibration” traceable to SI.
- Promote RADCALNET to be an operational network used for calibration, intercalibration and validation for the benefit of GEOSS.



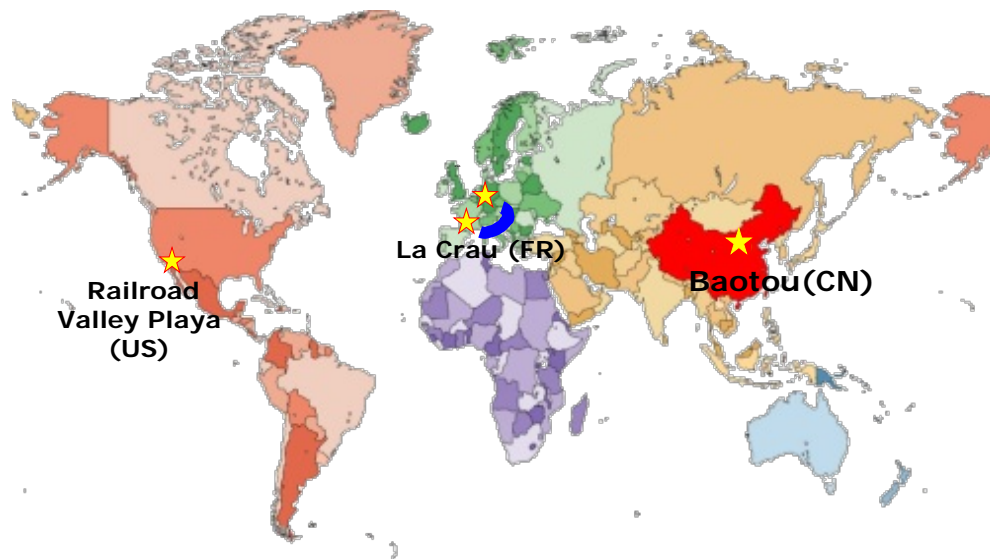
A scenic view of a lake with pink cherry blossoms in the foreground and green hills in the background. The text "Thank you!" is overlaid in a white, cursive font with a black outline.

Thank you!

➤ 3. High-frequency automated radiometric calibration for RadCalNet

Aims at an prototype of “global calibration” traceable to SI, CEOS/WGCV/IVOS WG agreed to set up the RADCALNET (**R**adiometric **C**alibration **N**etwork of **A**utomated Instruments). Three RADCALNET WG meetings have took place.

- Four sites provide data to RADCALNET:
 - ✓ **AOE Baotou site (China)**
 - ✓ La Crau site(France)
 - ✓ Railroad Valley Playa site (US)
 - ✓ ESA Site TBD (ESA/CNES)
- NPL (UK) provides support in harmonization, traceability, instrument calibration





➤ 4. Comprehensive Cal&Val site

Baotou
site

Support stringent aviation flight testing, radiometric calibration and in-orbit performance assessments for spaceborne optical / SAR payloads, Support remote sensing product validation.

Comprehensive

Radiometric
calibration

Geometric
calibration



Product
Validation

Image
quality
assessment